Molecular Crystals and Liquid Crystals
Publication details, including instructions for authors and subscription information:
http://www.tandfonline.com/loi/gmcl20

Conjugated Conducting Polymers as Components in Block Copolymer Systems

Lynne A. McCullough [a] & Krzysztof Matyjaszewski [a]
[a] Department of Chemistry, Carnegie Mellon University, Pittsburgh, PA, USA

Version of record first published: 28 May 2010

To cite this article: Lynne A. McCullough & Krzysztof Matyjaszewski (2010): Conjugated Conducting Polymers as Components in Block Copolymer Systems, Molecular Crystals and Liquid Crystals, 521:1, 1-55

To link to this article: http://dx.doi.org/10.1080/15421401003719951

Mol. Cryst. Liq. Cryst., Vol. 521: pp. 1–55, 2010

ISSN: 1542-1406 print/1563-5287 online
DOI: 10.1080/15421401003719951

Taylor & Francis
Taylor & Francis Group

Conjugated Conducting Polymers as Components in Block Copolymer Systems

LYNNE A. McCULLOUGH AND
KRZYSZTOF MATYJASZEWSKI

Department of Chemistry, Carnegie Mellon University,
Pittsburgh, PA, USA

Inducing nanostructure in conducting polymers and organically-derived nanostructured carbons provides additional control over their physical and electronic properties. These nanostructures have previously been produced by lithographic methods such as e-beam lithography, ion lithography and patterning involving pre-prepared masks. Self-assembly based on block copolymer self-segregation is another method for inducing nanostructures, one that contains a great deal of flexibility in the means of structure formation. Simply incorporating conducting moieties into one segment of a block copolymer via block extension or coupling is one primary strategy. Templating the conducting material or its precursor with block copolymer micelles and membranes, particularly when one segment of the copolymer exhibits affinity with the conducting polymer, is another heavily utilized method. This review discusses the use of block copolymers prepared by controlled radical polymerization as a tool for inducing nanostructure in conducting materials, from conducting polymers such as polythiophene and polypyrrole to carbon derived from organic polymer precursors such as resorcinol and polyacrylonitrile. Dividing principles include the type of conducting material, the method of self-assembly, the method of polymerization, and the block copolymer architecture.

Keywords ATRP; block copolymers; conducting polymers; controlled radical polymerization; nanostructured carbon; templating

Introduction

Conducting polymers with conjugated backbones have been tested in a wide range of applications since the discovery of their electrical potential in 1977 [1]. Polyacetylene was the first polymer of this type to be investigated, though it was quickly followed with polythiophene [2], polyphenylenevinylidene (PPV) [3,4], polyaniline (PANI) [5,6], and polypyrrole (PPY) [7,8], among a wide variety of other conjugated polymeric materials and their derivatives. These conjugated materials are inherently semiconducting, possessing a significant HOMO-LUMO band gap that limits electron mobility along the backbone. In order for this conjugated backbone (Fig. 1a) to become conducting, charge must be injected by a method known as

Address correspondence to Krzysztof Matyjaszewski, Department of Chemistry, Carnegie Mellon University, Pittsburgh, PA 15232, USA. Tel.: 412-268-3209; Fax: 412-268-6897; E-mail: km3b@andrew.cmu.edu

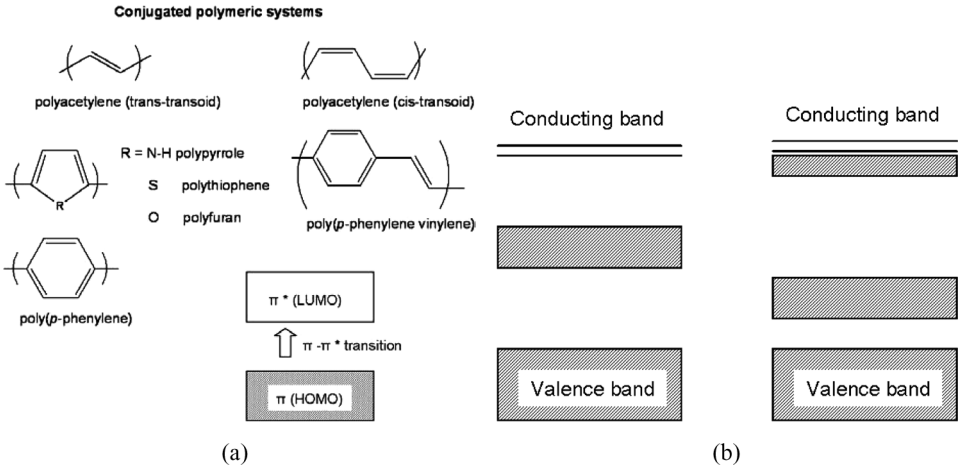

Figure 1. (a) A sampling of conducting polymers and the band gap and transition that gives their conducting properties (b) (left) Band structure for a soliton (right) band structure for a bipolaron formed from the combination of two polarons.

'doping' [9]. Doping can be either chemical or electrochemical; the polymer backbone is distorted around the charge carriers, which may be positively or negatively charged, depending on the mechanism of doping (Fig. 2). Solitons and polarons are chiefly differentiated by both the chemical changes they make in the polymer backbone; solitons are the boundary separating two regions of the polymer with different π-bond phases, while polarons (and bipolarons) are the boundary between quinoid-type and non-quinoid regions of conjugation [10]. The energy diagrams are different, as well, as solitons result in only one mid-gap state, while bipolarons (which result from the combination of two

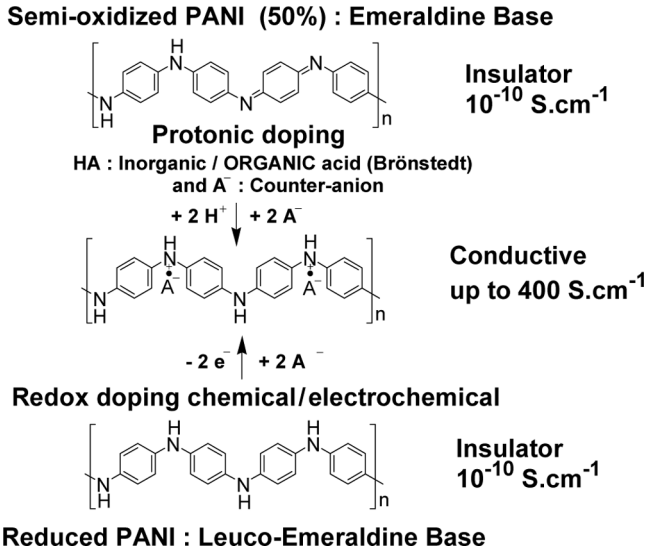

Figure 2. PANI doping via chemical and electrochemical means from emeraldine and leucoemeraldine base.

equal-energy polarons) exhibit two mid-gap states with a secondary gap energy in between them (Fig.1b). Regardless of the type of charge carrier in the polymer, the primary mechanism of conduction involves variable range hopping due to the mix of ordered crystalline regions and disordered amorphous regions in most conducting polymer materials and blends, which prohibits the existence of metallic conductivity.

While conducting polymers are highly desirable due to their low cost, easy synthesis, and highly conductive nature after proper processing, there are a few difficulties that have frequently prevented their wide-scale application [11]. Several properties of these polymers have highly influenced their potential utility in electronics applications, among these their stability (or lack thereof) in ambient conditions, the infusibility and poor solubility that arises from the highly conjugated backbone, and the brittle quality of the processed materials. Some of the earliest attempts at improving solubility involved the substitution of large organic groups (particularly long alkyl chains, though other functionalities were also included) onto the conjugated backbone [12,13]. While this did result in improved solubility, the electronic properties of such substituted polymers were often degraded based on electron withdrawing effects or loss of planar conformations in the backbone, both of which affect the mobility of the charge carriers [14]. Additionally these substituted groups did little to offset the brittleness of the processed materials.

A second approach to improving both the solubility and mechanical properties involves copolymerization of conducting materials with low-T_g amorphous polymers. Block copolymerization in particular allow the incorporation of a soluble segment that also possesses physical properties significantly different from those of the conjugated backbone while also providing a mechanism for self-organization into nanostructured materials. These nanostructures may also result in improved performance in the application of these materials, particularly in the case of photovoltaic devices. In addition to linear block copolymers, graft block copolymers have also been used to obtain unique structures with specific properties geared toward a variety of applications. Block copolymers without conducting polymer segments have also been successfully used as templates for discrete conducting nanoobjects, either as self-assembled porous membranes for nanorod synthesis or micellar templates for more complicated structural systems.

Linear Block Copolymers

Anionic Polymerization of the Amorphous Block

The earliest attempts at synthesis of linear block copolymers containing both conducting and amorphous segments began with the anionic polymerization of styrene using *sec*-butyllithium followed by end-capping with a functionalized thiophene such as 2,5-dibromothiophene [15]. This was then chain-extended with thiophene under chemical conditions (using $FeCl_3$ as the oxidant and dopant), resulting in films with morphologies ranging from spherical monolayers to fibrillar films, depending on the ratio of PS to PHT. Conductivities as high as 60 S/cm were observed: a moderate decrease from the conductivity of pure polythiophene, which ranges from several hundred to several thousand S/cm, depending on polymerization and processing conditions. Chemical polymerization, for example, produces lower conductivity materials than electrochemical polymerization. Similar block copolymers were prepared via the use of dibromodithiophene as the PS-capping

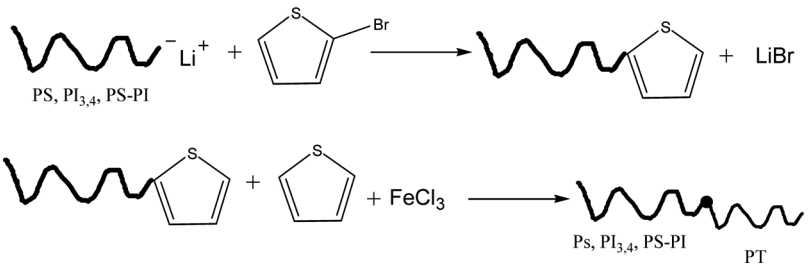

Figure 3. Block copolymers from thiophene end-capped anionic macroinitiators [18].

agent [16]. Additional structural studies on these PS-b-PHT copolymers by X-ray and neutron-scattering in both solution (CS_2) and in bulk demonstrated the formation of spherical aggregates with an average diameter of 75 nm, though after doping with $NOBF_4$ this aggregation disappeared due to the extended conformation of doped polythiophene [16,17]. Terpolymers with PS and polyisoprene (PI) were prepared by essentially the same method, utilizing anionic polymerization to prepare PS and PS-b-PI living anionic polymers that could be terminated by a dibromo-functionalized thiophene (Fig. 3). No conductivity results were given, but the PDI of these materials was <1.1 even after addition of P3HT, a significant improvement over previous block copolymers [18]. A different method, using aldehyde-functionalized oligothiophene as an end-cap for anionic polystyrene, was also developed. The oligothiphene nonamers were prepared by step-wise coupling using butyllithium and brominated 3-hexylthiophene, followed by a Vilsmaier reaction to attach an aldehyde end group (Fig. 4). These oligomers were then reacted with living polystyrene anions to produce the block copolymers with low polydispersities (1.1–1.12), though no phase separation was observed by TEM due to the low molecular weights of the oligothiophene block ($\sim$3000 g/mol) [19].

Triblock copolymers containing polythiophene were also prepared from an anionically-polymerized PS moiety (Fig. 5). The end-capping unit in this case was a 1-(4-((*tert*butyldimethylsilyl)-oxy)phenyl)-1-phenylethylene moiety that was then

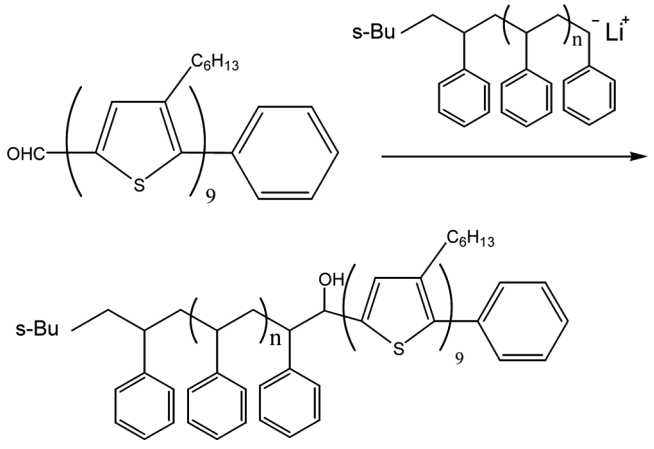

Figure 4. End-capping of anionic PS with aldehyde-functionalized PHT oligomers [19].

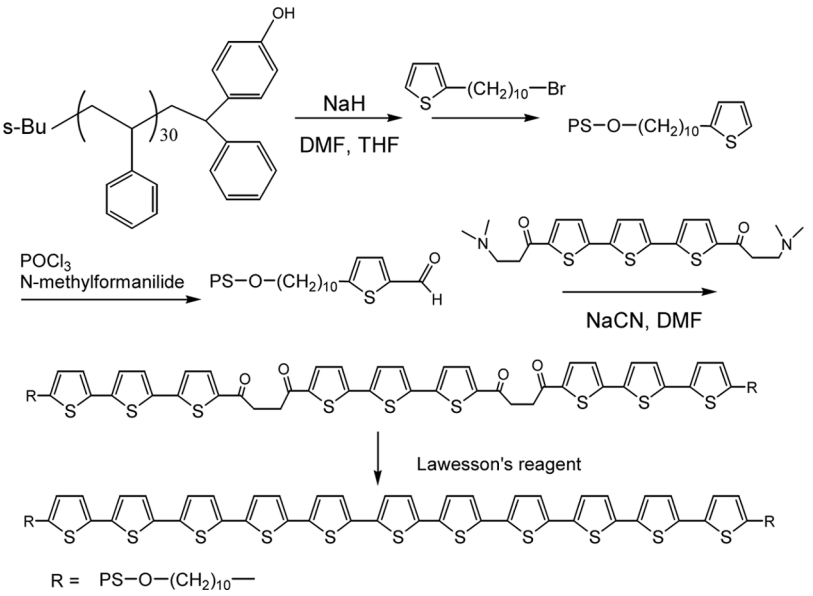

Figure 5. Triblock PS-b-PHT-b-PS copolymers from anionically-prepared PS [20].

deprotected with $Bu4N^{+}F^{-}$ to give a 4-hydroxyphenyl terminal group [20]. This group was reacted with 5-(10-bromodecyl)-2,2′:5′,2″-terthiophene. Formylation and subsequent Stetter coupling between two equivalents of the polystyrene/α-terthiophene and 5,5″-bis[3-(dimethylamino)propionyl]-2,2′:5′,2″-terthiophene, followed by a reaction with Lawesson's reagent resulted in formation of the triblock copolymer with an undecithiophene central block and bracketing PS blocks of DP = 30. As-cast films exhibited egg-shaped aggregates 14 nm in diameter that consisted of approximately 60 polymer chains, though increasing the thiophene content above 11 wt% may induce formation of rod and lamellar-like conducting domains.

The catalyst-transfer polycondensation-based Grignard metathesis (GRIM) [21–24] method (with nickel), discovered by the McCullough group, allows for easy preparation of poly(3-hexylthiophenes) (and other PTs) with controllable molecular weights and regioregularity of head-to-tail coupling. These polymers can also be easily modified via a variety of chemistries in order to obtain a range of α-end functionalities, including vinylic moieties. These vinyl groups can be activated using *sec*-butyllithium to become anionic polymerization initiating functionalities, allowing for the subsequent block extension of the polythiophene with vinylic monomers (Fig. 6) such as polystyrene [25] or poly(2-vinylpyridine) [26]. End-capping of the ω-end improves the block extension, because it prevents lithium-halogen exchange with the *sec*-butyllithium and thus removes the possibility of different lithiations at either end of the polymer. Polydispersities of these materials were 1.3, while the nanostructures as determined by TEM and X-ray were primarily spheres and cylinders for low thiophene compositions (<14 wt% PT), the expected behavior from coil-coil block copolymers. Higher % polythiophene resulted in more ordered structures, such as hexagonal close-packed cylinders or lamellae, while at > 50 wt% the morphology changed to nanofibers, largely due to the extensive π-π stacking in the polythiophene chains which were capable of overcoming the long-range order of the nanostructures [26].

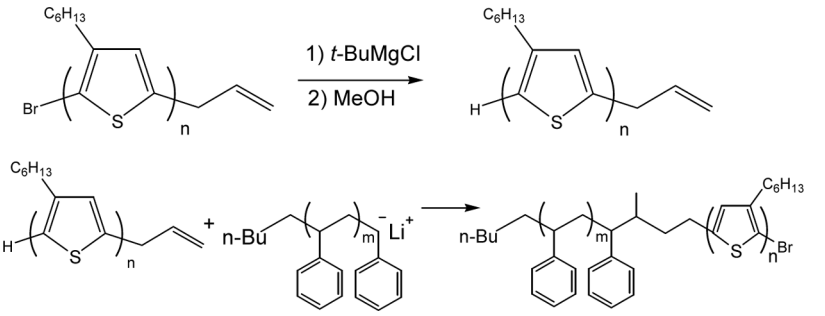

Figure 6. Block copolymers from allyl-functionalized P3HT via end-capping with anionic PS [25].

Controlled Radical Polymerization of the Amorphous Block: ATRP

With the development of alternative controlled polymerization methods for preparing amorphous polymers, primarily those utilizing radical chemistry [27–32] like atom transfer radical polymerization (ATRP) [33–39], nitroxide mediated polymerization (NMP) [40–43], and degenerative transfer processes such as reversible addition-fragmentation chain transfer (RAFT) [44–46], the potential for easy production of conjugated-amorphous block copolymers increased [47–54]. They can include polymers with interesting non-linear architecture and controlled composition [55–62]. Especially interesting is transformation of end groups in various polymers and using ATRP as the first or as the second polymerization technique [63–71]. The easiest and earliest method was utilized by the McCullough group, involving the use of the Grignard metathesis (GRIM) [21–24] method to prepare bromine-terminated poly(3-hexylthiophenes) that were reacted with a thiophene derivative containing a protected hydroxyl functionality using [Ni(dppp)Cl_2] (dppp = propane-1,3-diylbis(diphenylphosphane)). After deprotection the hydroxyl group was modified with 2-bromopropionyl bromide to create an ATRP initiating site as the terminal group for the P3HT (Fig. 7). This macroinitiator was then extended with styrene and methyl acrylate using CuBr/N,N,N′,N″,N″-pentamethyldiethylenetriamine (PMDETA) as the ATRP catalyst [72]. Similar techniques were used to be prepare difunctional P3HT macroinitiators that led to triblock copolymers (Fig. 8). The initial polythiophene was debrominated using Grignard metathesis and quenched with water. A Vilsmaier reaction on the subsequent polymer followed by reduction with $LiAlH_4$ gave P3HT with a dihydroxy functionality that was reacted with 2-bromopropionyl bromide to give the ATRP initiator-functionalized moieties. After oxidation with I_2 vapor these polymers gave conductivities of 3–5 S/cm with P3HT contents of ~40–50 wt% (P3HT $M_n \sim 17{,}000$ g/mol), while the observed morphologies were uniformly conducting nanowires as imaged by tapping mode AFM [72].

A simpler procedure for the modification of P3HT to ATRP macroinitiators was developed in 2005. This method used an allyl bromide modified to a Grignard reagent as an end-capping functionality for the brominated P3HT chain (Fig. 9). The hydroboration/oxidation of this vinyl functionality resulted in a hyroxy-terminated P3HT that could be reacted with 2-bromopropionyl bromide to form an ATRP initiator [73]. Polymerization of both methyl acrylate and *t*-butyl acrylate

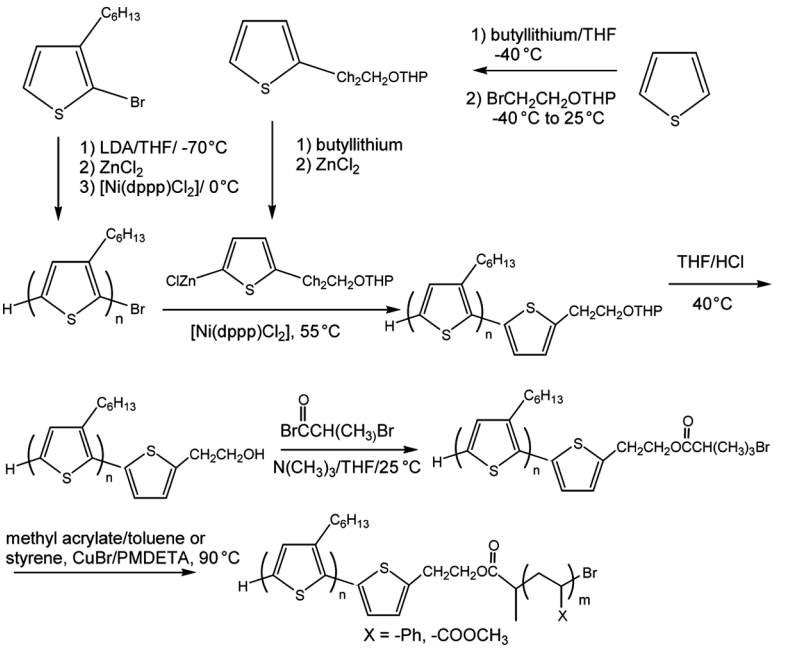

Figure 7. Block copolymers of P3HT and polyacrylates from a P3HT macroinitiator functionalized by an ATRP initiating site [72].

using these P3HT macroininitiators was accomplished using CuBr/PMDETA in 50:50 v% toluene at 80 and 90°C respectively, resulting in low PDI block copolymers (<1.3) that formed densely-packed smooth films drop-cast from toluene, unlike the cracked and brittle films prepared from pure P3HT. These polymers exhibited conductivities approximately one order of magnitude higher than those prepared by the previous method (~30 S/cm vs 3–5) at similar P3HT compositions (~50 wt%), and also exhibit field-effect mobilities as high as 0.048 $cm^2V^{-1}s^{-1}$ (0.084 $cm^2V^{-1}s^{-1}$ for pure P3HT) [74]. An additional benefit during synthesis is that the functionality on

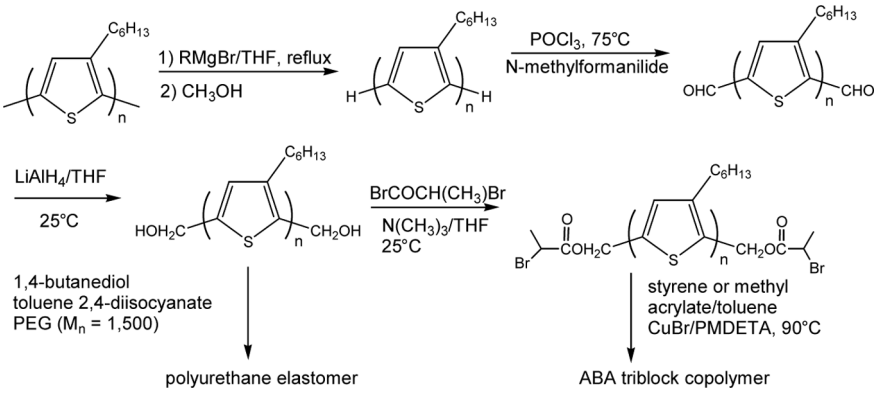

Figure 8. Triblock copolymers of P3HT and polyacrylates utilizing a dihydroxy-functionalized P3HT macroinitiator modified with an ATRP initiating site [72].

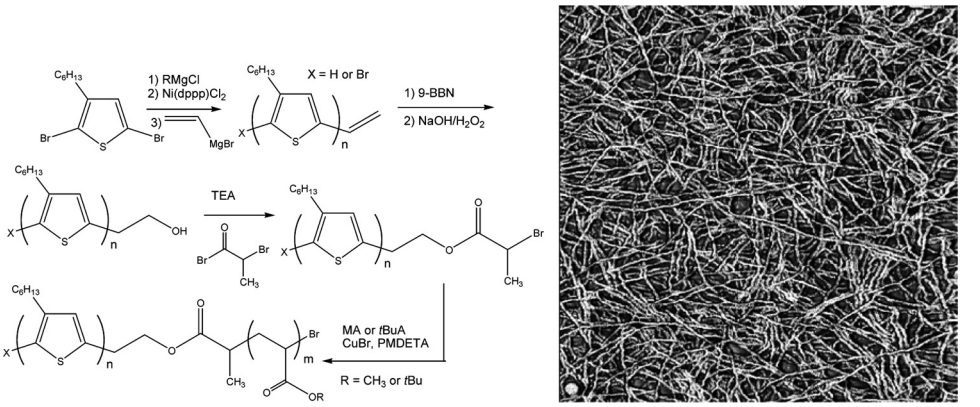

Figure 9. (l) Synthesis of ATRP macroinitiator and subsequent block extension from P3HT (r) nanowires of PS-b-P3HT cast from toluene [73].

the ω end of the P3HT can be either H or Br without interfering with the polymerization, unlike the difficulties experienced under similar conditions when block extending via anionic polymerization.

This same procedure was also used to prepare PS-b-P3HT and PBA-b-P3HT as components in volatile organic compound vapor sensors, where the nanowire morphology of the block copolymers in drop-cast films was again confirmed [75] (Fig. 10). Polymethacrylates were also prepared by this method, though due to the bromoester used to functionalize the P3HT (which forms an acrylate-equivalent radical), CuCl was used instead of CuBr in order to promote halogen exchange [76] and thus retain control of the polymerization. Polydispersities were ~1.35 for methyl methacrylate, 1.55 for *t*-butyl methacrylate, and 1.60 for isobornyl methacrylate-based P3HT block copolymers. As with the prior block copolymers, these materials exhibited nanowire morphologies after drop-casting from toluene, though the conductivities were significantly lower (<0.1 S/cm), in part due to the lower content

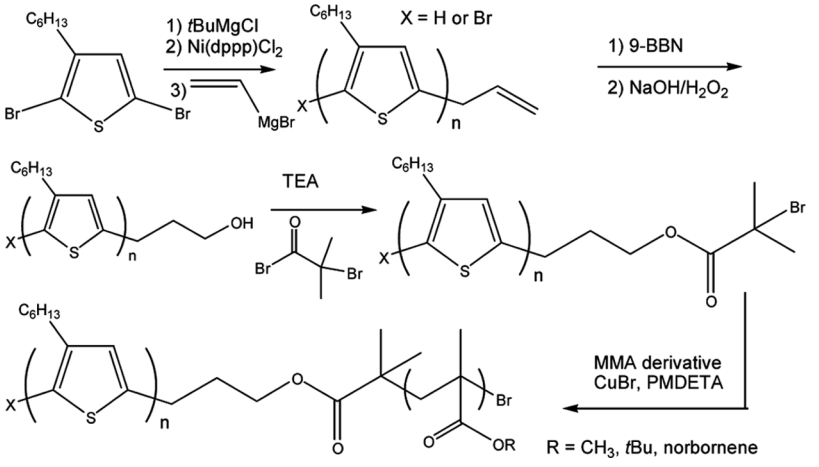

Figure 10. P3HT block copolymers containing polymethacrylates prepared by ATRP [75].

of P3HT in these materials (11.7–22.6 wt% P3HT) [77]. Block copolymers of P3HT and poly(*t*-butyl acrylate) were prepared by the same method; a subsequent hydrolysis step using trifluoroacetic acid and 1,4-dioxane resulted in the formation of amphiphilic block copolymers of P3HT and poly(acrylic acid) PAA. These materials exhibited the same nanofibrillar morphologies as previous P3HT-containing diblock copolymers, and obtained conductivities up to 1 S/cm with 72 wt% P3HT [78].

Butyl acrylate-containing P3HT block copolymers were also prepared by utilizing a thiophene-functionalized ATRP initiator prepared by reacting 2-thiophene methanol with 2-bromoisobutyryl bromide [79]. Block extension with *t*-butyl acrylate followed by polymerization of 3HT using $FeCl_3$ as the oxidant/dopant and subsequent purification resulted in diblock copolymers containing both P3HT and P*t*BA (Fig. 11). Triblock copolymers were also prepared by 'end-capping' a P3HT prepared via chemical polymerization with the compound used to make the ATRP initiator (2 equivalents), which was followed by the ATRP of styrene using CuBr/PMDETA. Additional purification was required in order to separate the diblock copolymers formed concomitantly during this reaction. Conductivities and solid-state morphologies for these materials were not reported.

This same group also investigated the utility of click chemistry as a means of preparing PS-b-P3HT copolymers, using an azide-functionalized ATRP initiator (3-azidopropyl-2-bromoisobutyrate) for the polymerization of PS with CuBr/bipyridine as the catalyst system [80]. The acetylene-substituted P3HT was prepared by end-capping the GRIM-prepared polythiophene with ethynylmagnesium bromide (Fig. 12). Click coupling between this P3HT and PS was unsuccessful due to the conjugation between the P3HT backbone and the alkyne group, limiting its ability to react with the azide functionality. Incorporating an alkyl spacer between the thiophene backbone and the alkyne group was more successful; α,ω-pentynyl-P3HTs were prepared using (5-chloromagnesio-1-pentynyl)trimethylsilane, followed by deprotection using tributylammonium fluoride (TBAF). Click chemistry was done

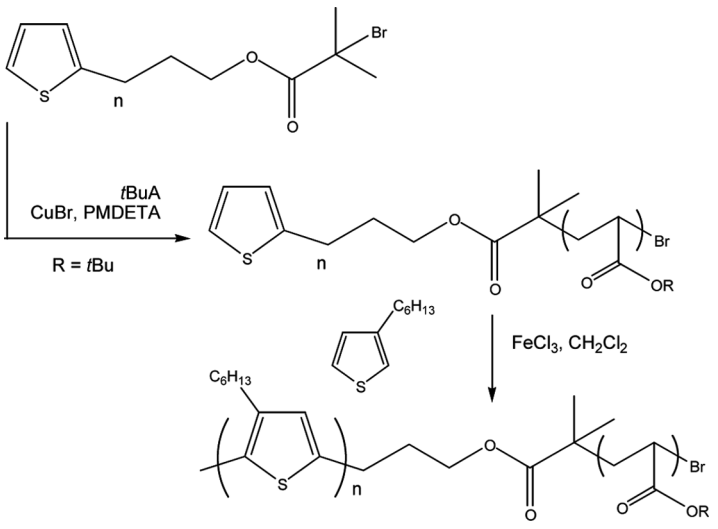

Figure 11. Block copolymers of P3HT and acrylate prepared from thiophene-functionalized ATRP initiators [79].

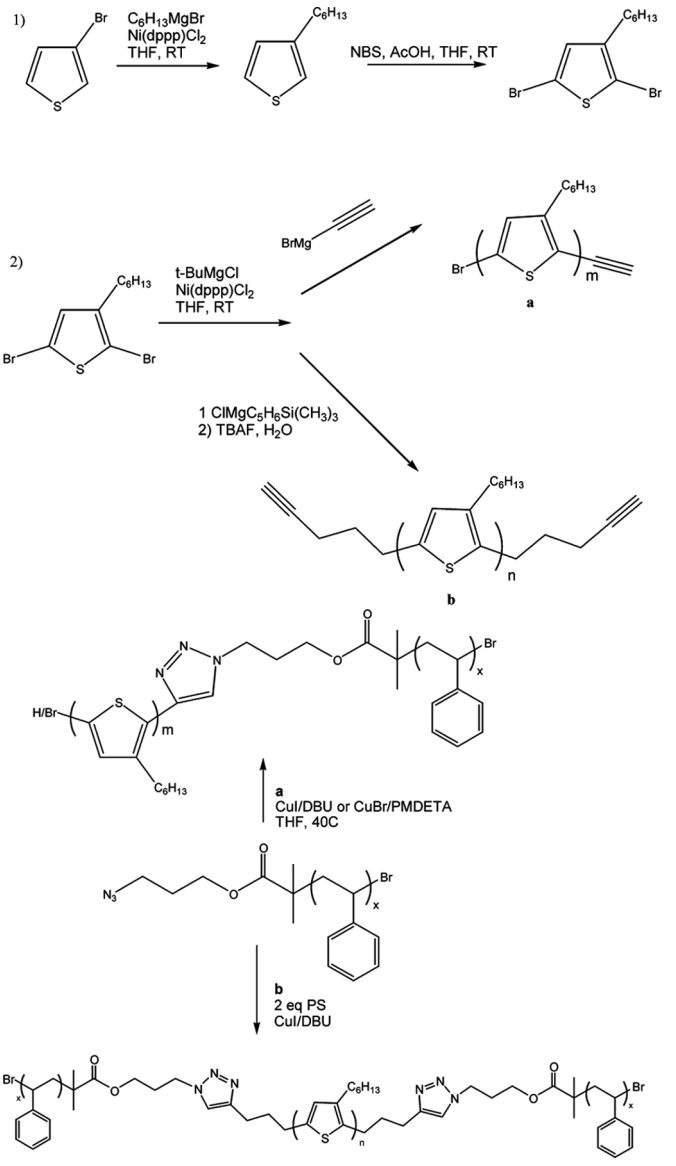

Figure 12. Click chemistry of an azide-modified PS with alkynyl-modified P3HT to prepare block copolymers [80].

to link the azide and alkyne functionalities into trialkylimides using CuI, and was successful according to ^{1}H-NMR and FTIR.

Toppare and Yagci used a similar procedure to prepare polypyrrole-containing block copolymers. A thiophene-functionalized initiator, N-trichloroacetyl-2-thiophenyl methyl carbamate was used with CuCl/4-4′-(5-nonyl)-2,2′-bipyridine (dNbpy) as the catalyst at 130°C to polymerize the methyl methacrylate (MMA) macroinitiator (15,000 or 28,000 g/mol, PDI 1.18 and or 1.14, respectively). A 1% solution of this polymer was used to coat the electrode for electrochemical

polymerization of polypyrrole (PPY) at $+1$ V vs Ag/Ag^+ in the presence of dopants toluenesulfonic acid (TSA) or sodium dodecyl sulfonate (SDS). Conductivities of these films were $\sim$8 S/cm on both the electrode and solution sides. Free radical polymerization utilizing a thiophene-functionalized initiator 4,4′-azobis(4-cyano-3-thiophenemethyl)pentanate (ACTMP) was used to prepare a styrene macroinitiator that was ostensibly difunctional due to termination of the polymerization by coupling (Fig. 13). Electropolymerization resulted in thin films with conductivities between 6 and 8 S/cm [81]. However, due to direct deposition of these film onto the electrode and the lack of directed initiation by the thiophene moiety on the macroinitiator, it is likely that the deposited films contained a mixture of block copolymer, cross-linked materials, and PPY homopolymer, or may have resulted in structures more like graft copolymers, which will be discussed in a subsequent section of this paper. Similar macromonomers were prepared using 2-pyrrolylethyl 2-bromo-2-methylpropionate as the initiator for the ATRP of MMA, *n*-butyl acrylate, *t*-butyl acrylate, styrene, 2-methoxyethoxy acrylate, poly(ethylene oxide) monomethacrylate, and a 6:4 copolymer of MMA:(dimethylamino)ethyl methacrylate using $NiBr_2(PPh_3)_2$ or CuBr/bpy as the catalyst [82] (Fig. 14). These end-functionalized polymers were extended with PPY using chemical or electrochemical polymerization techniques.

Oligofluorenes synthesized via Suzuki cross-coupling have also been functionalized with ATRP initiating sites at the chain end, particularly terfluorenes such as 2,7″-bis(4′-hydroxy-1,1′-biphenyl-4-yl)-9,9,9′,9′,9″,9″-hexahexyl-7,2′:7′,2″-terfluorene. Reacting this compound with chloropropionyl chloride resulted in the formation of an ATRP macroinitiator that was then extended with P*t*BA and PS using CuBr/PMDETA as the catalyst [83], and PHEMA [84] using CuBr/bipy as the catalyst (Fig. 15). Triblock copolymers from difunctional terfluorene initiators were prepared by a similar method. Polydispersities were low ($\sim$1.2) at low conversions and low amorphous polymer molecular weights ($<$10,000 g/mol), while higher conversions exhibited PDI ranging from 1.65–1.90. DSC measurements gave evidence for phase separation in these polymers, while honeycomb-like morphologies were observed from as-cast films of the PHEMA-based block copolymers using AFM [84].

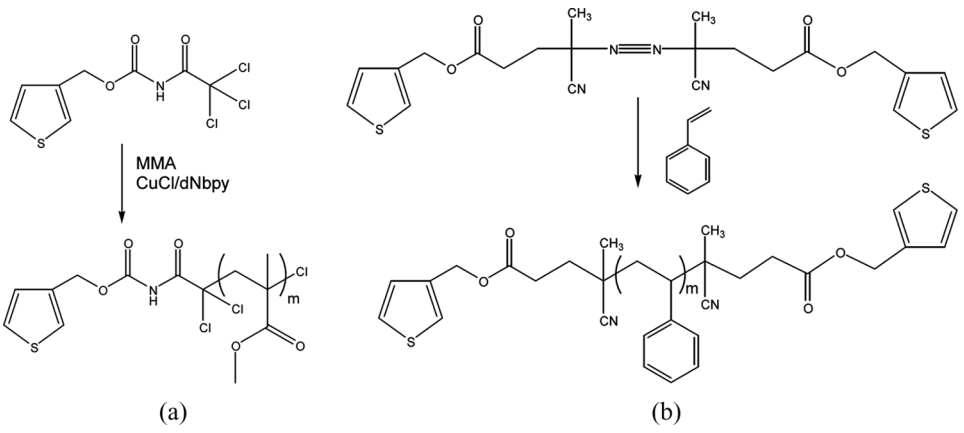

Figure 13. Thiophene-functionalized initiators as precursors to block copolymers containing an amorphous block and a conjugated polythiophene or polypyrrole block [81].

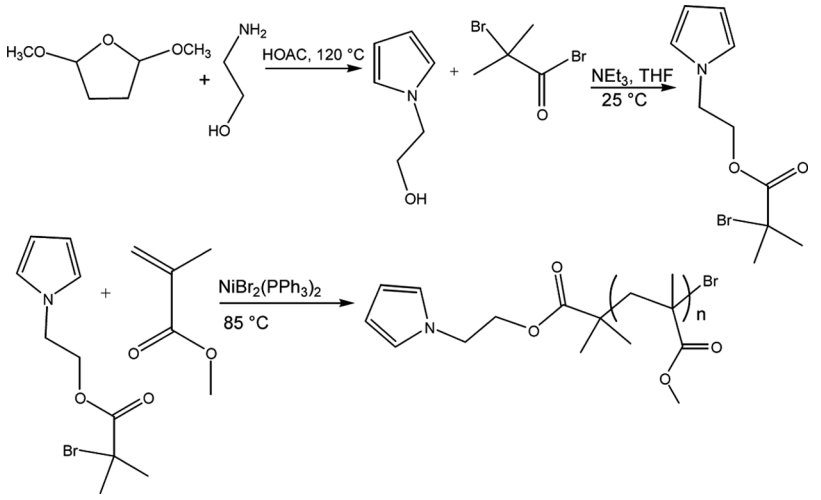

Figure 14. Pyrrole-functionalized ATRP initiator for the preparation of diblock copolymers of acrylates and PPY [82].

A longer oligofluorene hexamer, 4-(2,5-di(oligofluorenyl)-4-methoxyphenoxy)butan-1-ol (OFBOH), was used as a macroinitiator for the polymerization of the liquid crystalline monomer 6-(4′-cyanobiphenoxy)hexyl methacrylate by ATRP with CuBr/1,1,4,7,10,10-hexamethyl-triethylenetetramine (HMTETA) as the catalyst in *o*-dichlorobenzene (Fig. 16). These block copolymers had PDI <1.20, a smectic mesophase, and exhibited photoluminescence intrachain energy transfers in solution and interchain transfers in solid films [85].

Controlled Radical Polymerization of the Amorphous Block: NMP and RAFT

Nitroxide mediated polymerization (NMP) [40–42] was also used extensively in the preparation of rod-coil block copolymers containing a rigid conjugated segment. P3HT terminated in a hydroxypropyl group was reacted with either 3-benzylsulfanylthiocarbonylsulfanylpropionic acid chloride to form a trithiocarbonate RAFT agent or 2,2,5-trimethyl-4-phenyl-3-azahexane-3-oxy (TIPNO) to generate an alkoxyamine initiator (Fig. 17). The RAFT macroinitiator was extended with PS while the NMP alkoxyamine initiator was extended with polyisoprene. These block copolymers had PDI <1.5 for RAFT and <1.80 for NMP, with conductivities in the several S/cm range with ~40 wt% P3HT, while the morphology of drop-cast films was nanofibrillar, as seen previously with the block copolymers of P3HT prepared via ATRP [86].

An oligothienylenevinylene (3,4-dioctyl(2,5-thienylenevinylene)) (DO-PTV) (Fig.18) was prepared via a Horner-Emmons-Wadsworth condensation, capped with an aldehyde functionalized-thiophene, and reacted with a TIPNO-derivative via lithiation with *n*-butyllithium and subsequent reaction, identical to the method described by Hadziioannou *et al.* for the functionalization of polyphenylenevinylene (PPV) with a TIPNO-based initiating moiety (Fig. 19) [87]. This polymer was block extended with styrene and *p*-chloromethylstyrene to form a copolymer potentially suitable for further functionalization with a C_{60} moiety for use in photovoltaic

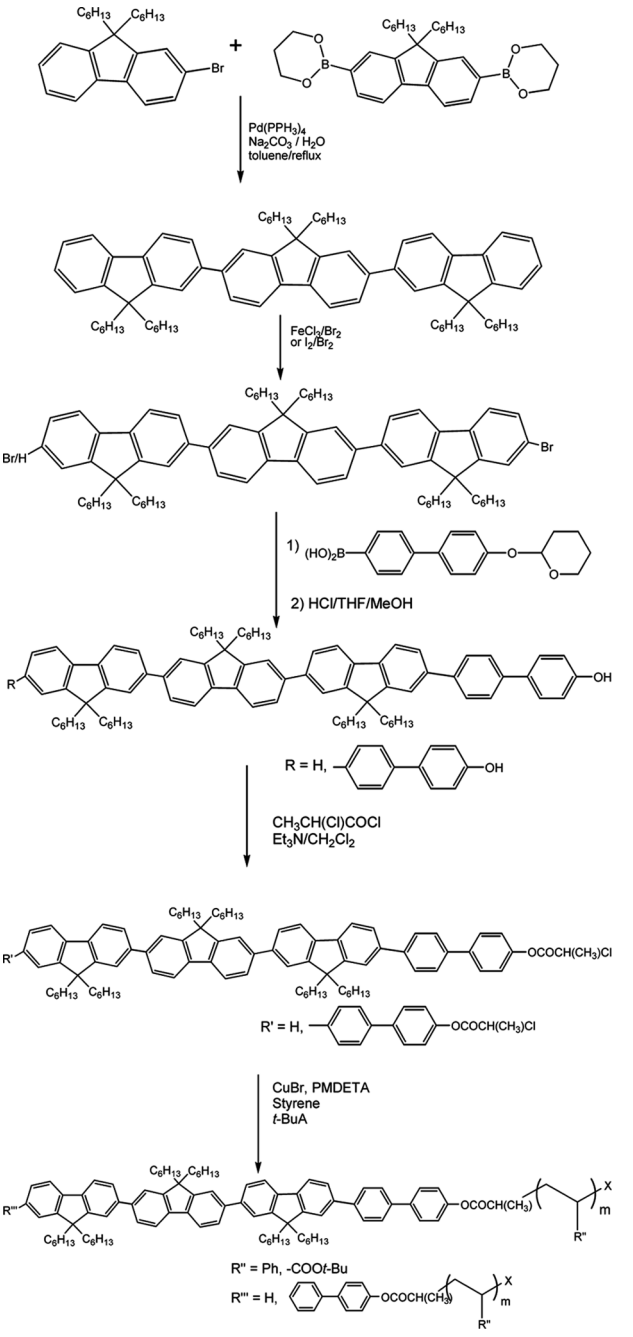

Figure 15. Synthesis of a difunctional oligofluorene ATRP macroinitiator and subsequent block extension with vinyl monomers [83–84].

applications [88]. Indeed, the majority of NMP-based preparation of rod-coil block copolymers contains P3HT or PPV as the donor block and C_{60} (or another acceptor functionality) as a component of the acceptor block. NMP is particularly useful for

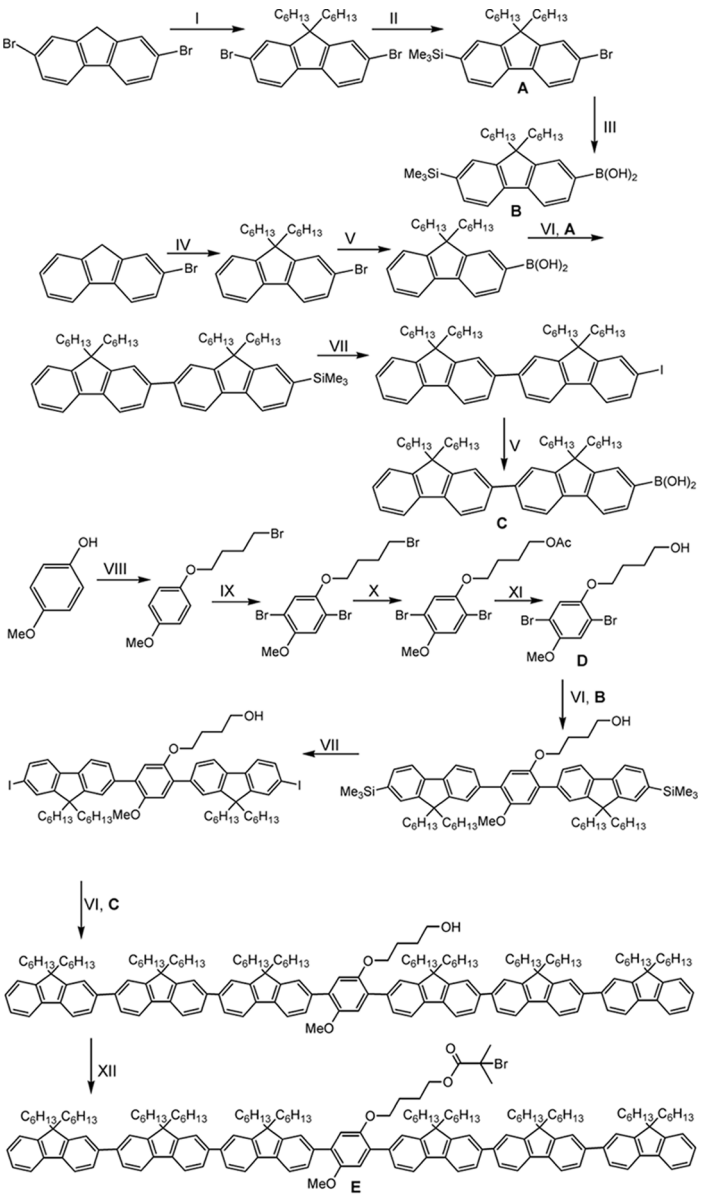

(a)

Figure 16. Oligofluorene modified with an ATRP initiating functionality for the preparation of diblock copolymers with liquid crystalline monomers [85]. (a) (I) DMSO, NaOH (w/w, 50%), 1-bromohexane, RT; (II) (1) *n*-BuLi, −78°C (2) $ClSiMe_3$, −78°C to RT (3) H_2O; (III) (1) *n*-BuLi, −78°C (2) $(i\text{-}PrO)_3B$, −78°C to RT; (IV) DMSO, NaOH (w/w 50%), 1-bromohexane, 70°C; (V) (1) *n*-BuLi, −78°C (2) $(MeO)_3B$, −78°C to RT (3) H_3O^+; (VI) $Pd(PPh_3)_4$, Na_2CO_3 (2 M aq.), 90°C; (VII) ICl, 0°C; (VIII) 1,4-dibromobutane, KOH, 90°C; (IX) Br_2 (3 M in $CHCl_3$), RT; (X) KAc, 70°C; (XI) (1) $Pd(PPh_3)_4$, Na_2CO_3 (2 M aq.), 90°C (2) KOH, RT; (XII) 2-bromoisobutyryl bromide, $N(CH_2CH_3)_3$, 0°C. (b) (I) 6-bromo-1-hexanol, K_2CO_3, 60°C; (II) DCC, DMAP, room temperature; (III) HMTETA, CuBr, 60°C.

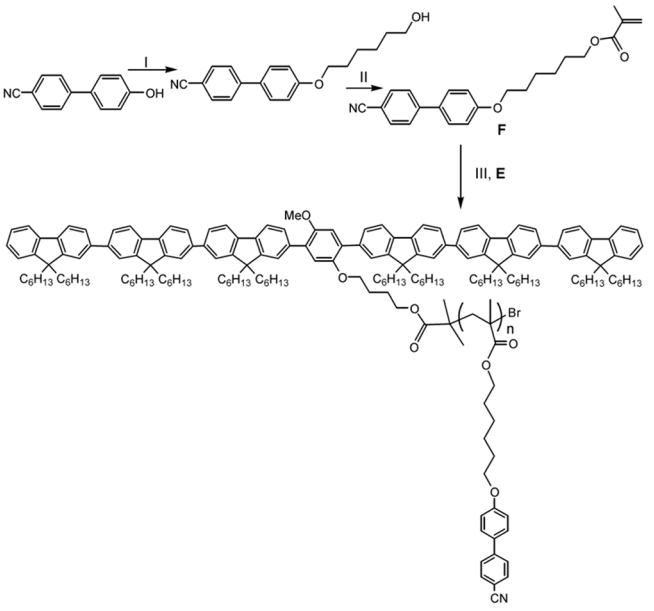

(b)

Figure 16 Continued.

these types of materials because there is no metal contamination to interfere with the functioning of a photovoltaic cell.

One of the earliest attempts at using donor-acceptor block copolymers as photovoltaic cell components involved precursors containing a 4-chloromethylstyrene (CMS) block (diluted with pure styrene in order to prevent crosslinking) that were functionalized with a C_{60} moiety using atom transfer radical addition (ATRA)

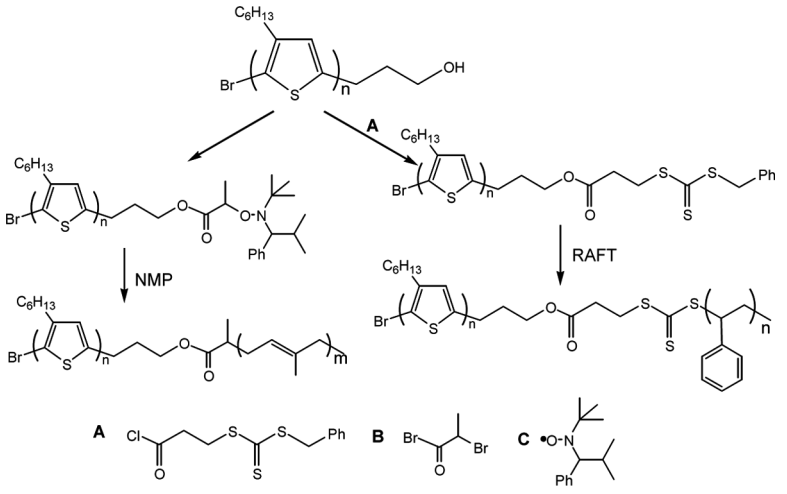

Figure 17. Modification of hydroxyl-functionalized P3HT into RAFT and NMP macroinitiators for block extension via controlled radical polymerization [86].

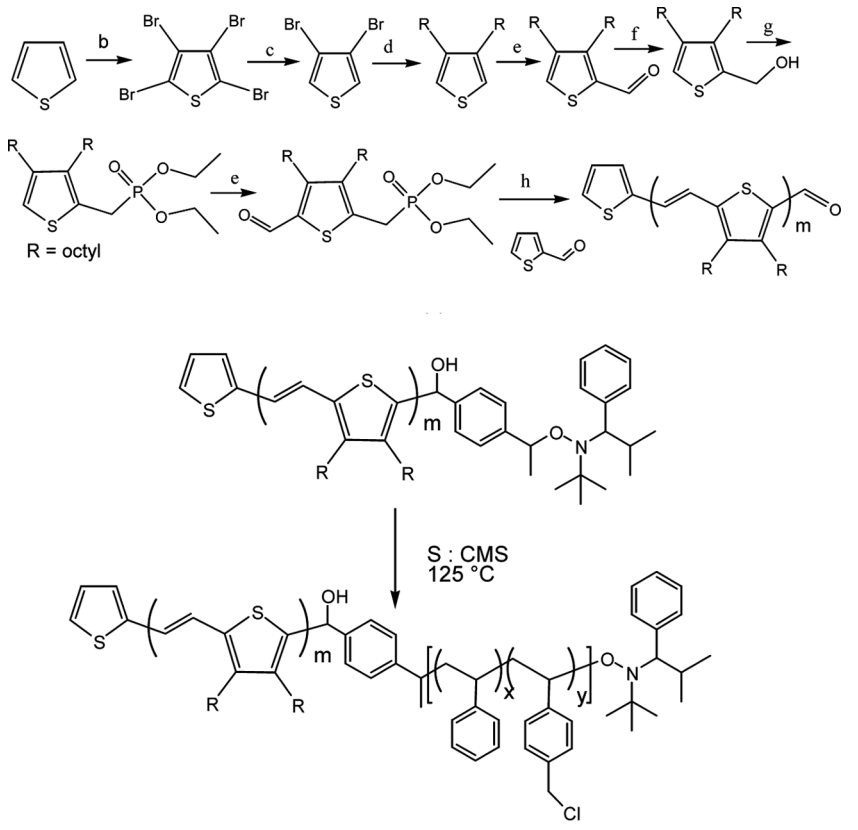

Figure 18. Preparation of DO-PTV and subsequent block extension via NMP [88]. (b) Br_2, AcOH, 80°C, 16 h; (c) Zn, H_2O/AcOH 7:3, room temperature, 2 h; (d) bromooctane, Mg, $NiCl_2$[dppp], ether, room temperature, 16 h; (e) POCl3, DMF, DCM, reflux, 5 h; (f) $NaBH_4$, DCM/methanol 1:1, 0°C, 3 h; (g) PBr_3, toluene/benzene 2:1, −30°C, 5 min and then $(OEt)_2$ P(O)H, NaH, THF, −30°C, 30 min and then reflux, 2 h; and (h) 2-thiophenecarbaldehyde (**13**), KOtBu, THF, room temperature, 24 h.

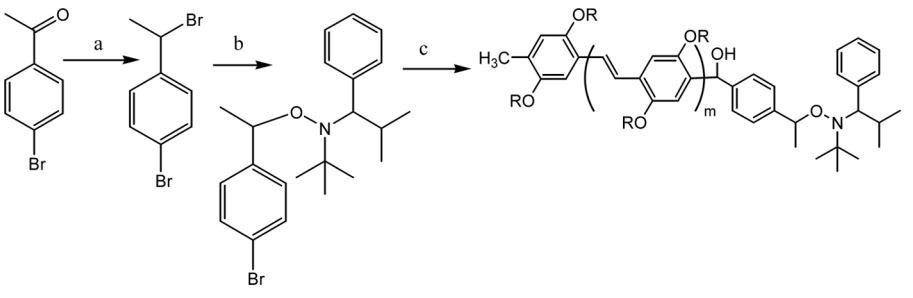

Figure 19. TIPNO-functionalization of linear PPV for preparation of an NMP macroinitiator [87]. (a) (1) $LiAlH_4$, diethyl ether, RT, 3 h; (2) PBr_3, toluene, pyridine, RT, 12 h; (b) TIPNO radical, CuBr, Cu, bipy, toluene, 75°C, 12 h; (c) (1) *n*-BuLi, diethyl ether, −40°C (RT; (2) aldehyde-terminated PPV, THF, 60°C, 2 h. RT.room temperature, bipy, 2,2′-bipyridine.

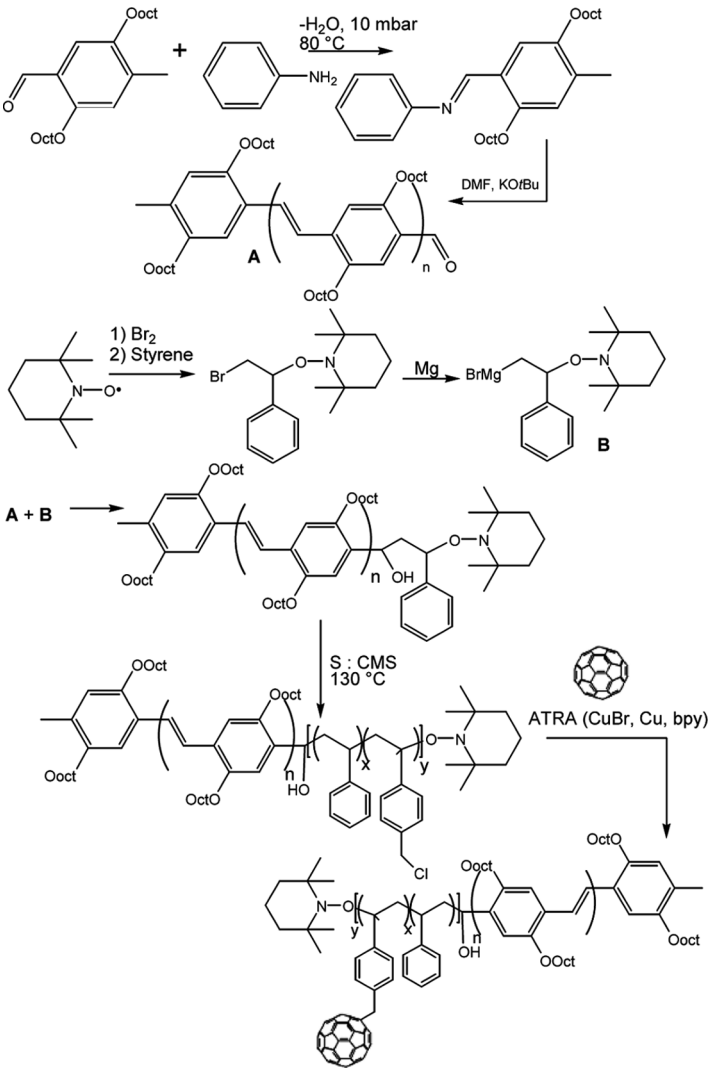

Figure 20. Synthetic scheme for DOO-PPV-*b*-P(S-*stat*-C_{60}MS) [89,90].

[89,90]. The block copolymer itself was prepared starting with the PPV block; in this case poly(2,5-dioctyloxy-1,2-phenylenevinylene) (DOO-PPV) was prepared using the Siegrist polycondensation, utilizing a strong base, as shown in Figure 20. The TEMPO initiating group was then reacted with the terminal aldehyde on the PPV, resulting in a macroinitiator that could be block-extended with styrenic monomers. When carbon sulfide (CS_2) is used as the processing solvent, a honeycomb-like morphology is formed. Processing from dichlorobenzene, however, results in materials with a more bicontinuous morphology. Luminescence in these materials is quickly quenched upon functionalization with C_{60}, while a similar response is not seen in the unreacted block copolymer.

A second method of block copolymerization has been reported by the same group [91,92]. This one utilizes (TIPNO) as the nitroxide-mediating functionality,

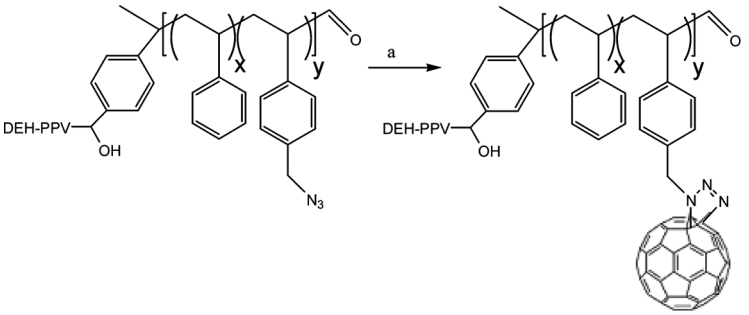

Figure 21. Functionalization of azide-functionalized chloromethylstyrene (CMS) with fullerene [40]. (a) Chlorobenzene, 60°C, 20 h. Triazoline reduced in dichlorobenzene at 130°C for 1 h, resultedin in [6,6] or [5,6] nitrogen-bridged fullerenes.

though the preparation of the PPV-based macroinitiator is identical to the above procedure in all other respects. The second variation is that click chemistry utilizing azides and acetylene functionalities replaced the ATRA coupling reaction to remove the potential for crosslinking during the C_{60} functionalization (Fig. 21), because no C_{60}-Cl bonds were formed, and thus there were no C_{60} radicals in the reaction system to serve as crosslinking sites. No optoelectronic properties were analyzed, though the prepared rod-coil diblock copolymers did exhibit lyotropic liquid crystalline behavior when irradiated with cross-polarized light.

Polythiophenes have also been used as the rod portion of these C_{60}-functionalized block copolymers [93,94]. The preparation of the polythiophene macroinitiator is similar to the preparation of the previously discussed PPV-based macroinitiator. The polythiophene was prepared with the GRIM method and the polymer end-capped with a Grignard reagent containing the TIPNO functionality (Fig. 22). This polymer was block extended with a statistical copolymer of *n*-butyl acrylate and chloromethylstyrene (CMS) using nitroxide-mediated polymerization, and the C_{60} moiety was attached using azide-based click chemistry. Again, the optoelectronic properties of these polymers were not investigated; neither were their potential as device components. However, the photoluminescence spectra of both the initial copolymer and the C_{60}-modified copolymer were obtained, and there were significant amounts of fluorescence quenching for the fullerene-containing materials in solution, while in the thin-film materials quenching was almost complete. A second D-A P3HT was prepared by the GRIM method, end-capped with allylmagnesium bromide and functionalized with a TIPNO alkoxyamine, based on Hadziioannou's procedure. This functionalized P3HT was used as a macroinitiator for the polymerization of perylene diimide acrylate at 125°C in 1,2-dichlorobenzene (Fig. 23). This block extension resulted in the preparation of block copolymers with PDI 1.2–1.4, complete fluorescence quenching, and an observed power conversion efficiency (post-annealing under toluene-chloroform vapor) of 0.49% [95].

Ring-Opening and Ring-Opening Metathesis Polymerization

CRP is not, however, the only method available for preparing block copolymers as components in solar cells. Fréchet's group recently prepared block copolymers by ROMP with a C_{60}-functionalized norbornene (Fig. 24) [96] and polythiophene,

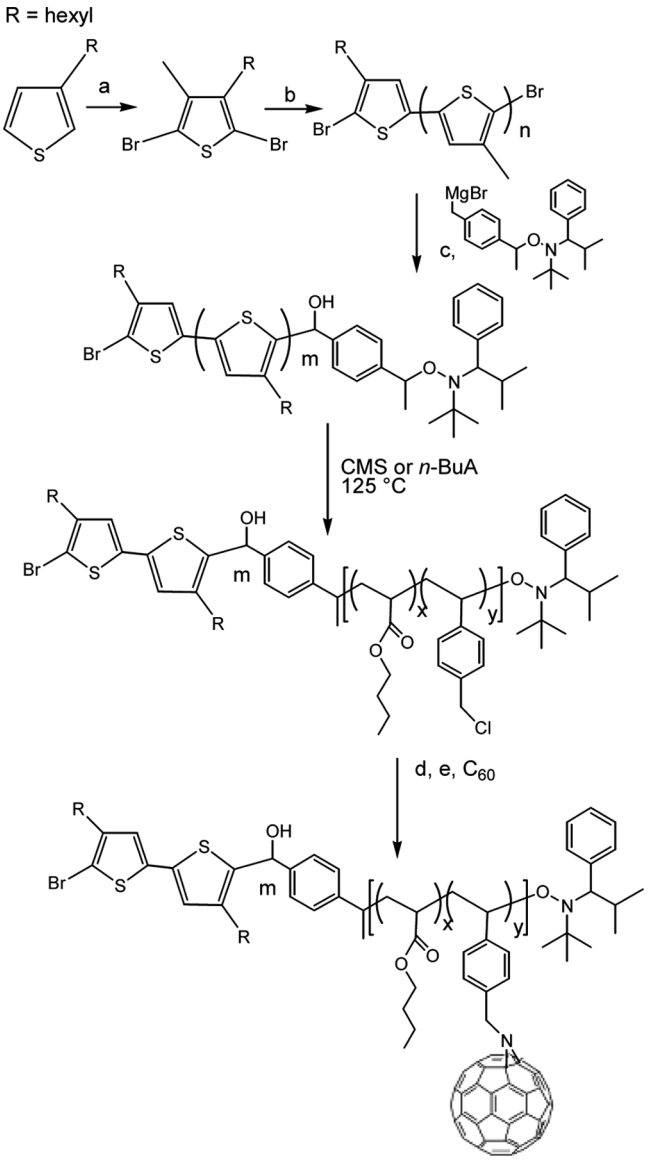

Figure 22. Preparation of P3HT-*b*-P(BA-*stat*-CMS) and subsequent functionalization with C_{60} [42]. (a) NBS, $CHCl_3$/AcOH 1:1, RT; (b) (1) *t*-BuMgCl, ether/THF, RT (2) $Ni(dppp)Cl_2$, ether/THF, RT; (c) ether/THF, RT; (d) NaN_3, DMF, 50°C; and (e) dichlorobenzene, 60°C then 120°C.

and then used these materials as compatibilizers to lower the phase separation and improve the performance of physical blends of optoelectronic polymers and PCBM [97]. Polythiophene was end-capped with a norbornene functionality and used in conjunction with the C_{60} monomer to prepare amphiphilic block copolymers containing both donor and acceptor moieties. Pre-annealed systems of pure P3HT/PCBM exhibited no phase separation at the scale of 50 nm. This diminished on addition of 5 wt% P3HT-b-C_{60} block copolymer and became undetectable by

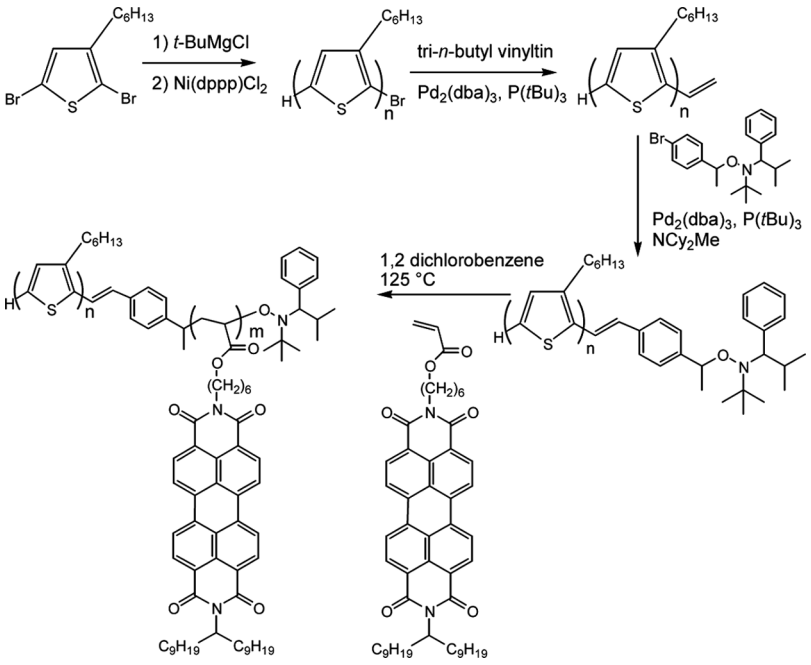

Figure 23. Preparation of TIPNO-functionalized P3HT and subsequent block extension with perylene diimide acrylate via NMP (5% excess TIPNO) [95].

TEM after addition of 17 wt% of the block copolymer, indicative of reduced surface tension between the system. The device performance based on these compatibilized materials exhibits significant improvement in efficiency (η_e) compared to blends of P3HT and PCBM without the addition of a block copolymer, particularly at high annealing times (annealing temp. = 140°C), meaning that the extended performance of these materials in solar cells should be similarly improved. ROMP has also been used in the preparation of P3HT-b-poly(ethylene) via block extension with cyclooctene [98] (Fig. 25).

Ionic ring-opening polymerization has also been used to prepare P3HT-based block copolymers with a degradable insulating segment that can promote organization of the conducting polymer before being removed. Using polylactide (PLA) as the degradable polymer, allyl-functionalized P3HTs prepared by the GRIM method were subjected to hydroboration/oxidation to form hydroxypropyl functionalities at the chain end (Fig. 26). Lactide was then polymerized using $AlEt_3$ in equimolar amounts to the hydroxypropyl group to prepare atactic PLA-b-P3HT and PLA-b-PDDT (poly(3-dodecylthiophene)); the latter polymer was useful as the T_m is lower for larger alkyl chains, thus making the thermal degradation of PLA an easier prospect where the T_m of PAT is lower than the decomposition temperature of PLA (<220°C) [99].

Oxidative Coupling of Conjugated Conducting Polymers and Amorphous Polymers

Multiblock copolymers containing poly(ethylene oxide) (PEO) and polythiophene (PT) have been prepared using bromothiophene or dibromo-bithiophene-functionalized PEO in a Stille cross-coupling with 2,5-bis(trimethylstannyl)thiophene

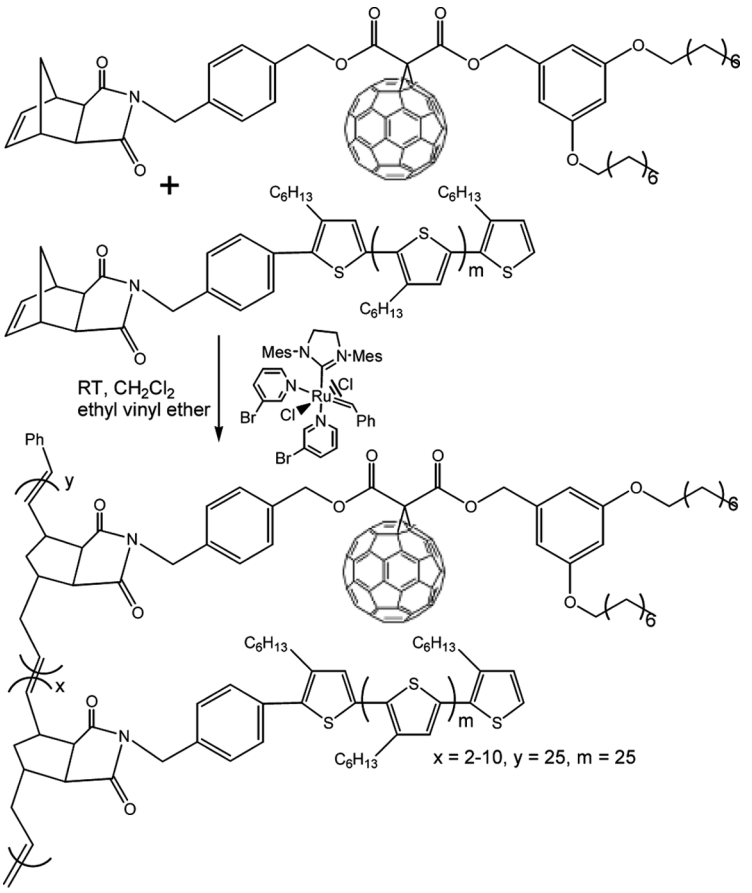

Figure 24. Preparation of C_{60}-containing block copolymer using ROMP [96].

or 5,5′-bis(trimethylstannyl)-2,2′-bithiophene [100] (Fig. 27). These materials exhibited behavior similar to that of cross-linked rubbers when hexathiophenes were used, demonstrated parallel face-to-face stacking in UV with a shift in the maximum from 448 nm to 410 nm from dioxane to 83% water solution), and exhibited lamellar orientation in thin solid films cast from dimethylformamide (DMF) [101]. Suzuki

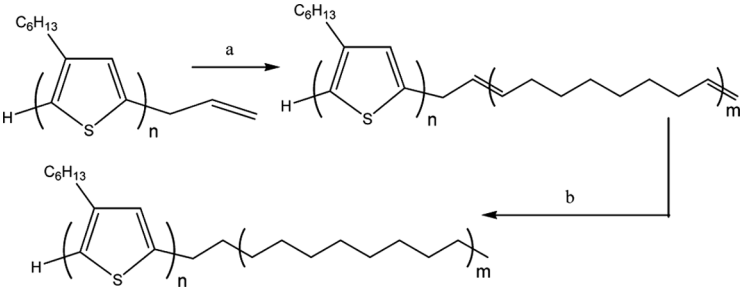

Figure 25. P3HT block extended with polyethylene using ROMP [98]. (a) Cyclooctene, Ru-(H_2IMes)Cl_2PCy_3(=CHPh), chlorobenzene, 55°C, 24 h. (b) *p*-Toluenesulfonhydrazide,*p*-xylene, 130°C, 8 h.

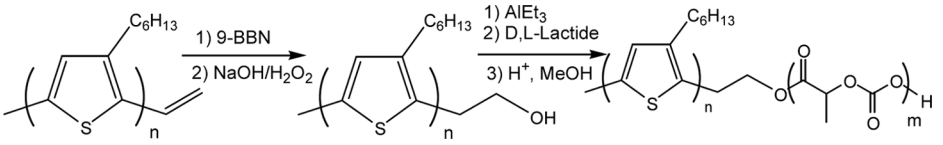

Figure 26. P3HT extended with PLA via ROP with $AlEt_3$ [99].

cross-coupling has also been utilized to make PEO-b-PT block copolymers, though they exhibited poor solubility even in DMF and chloroform [102] (Fig. 28). Block copolymers containing polyaniline and PEO have also been prepared from diamine-functionalized PEO via emulsion polymerization with dinonylnaphthalene sulfonic acid (DNNSA) and 2-butoxyethanol. Block copolymers containing poly(propylene oxide) (PPO), poly(dimethylsiloxane) (PDMS), and poly(acrylonitrile-co-butadiene) were similarly prepared. Conductivities were uniformly low (10^{-6} S/cm), though they were soluble in solvents such as toluene or xylene [103]. Diblock copolymers

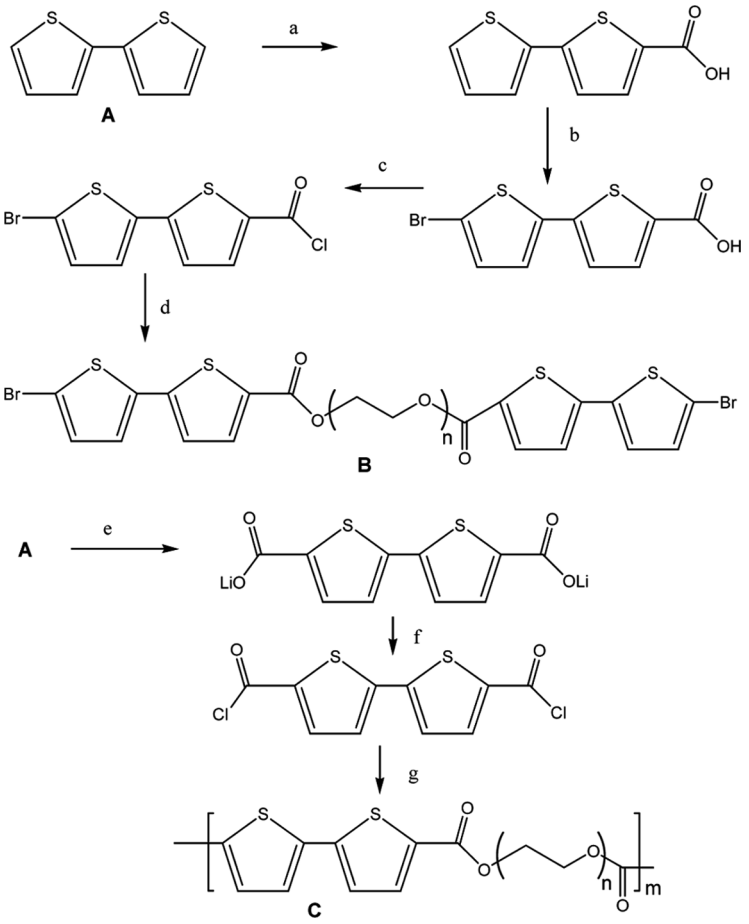

Figure 27. Preparation of PEO-b-PT via coupling reactions [100]. (a) THF, n-butyllithium, CO_2; (b) DMF, NBS; (c) $SOCl_2$; (d) toluene, pyridine, PEO ($M_n \sim 2000$). (e) THF, *n*-butyllithium, CO_2; (f) $SOCl_2$; and (g) PEO ($M_n \sim 2000$).

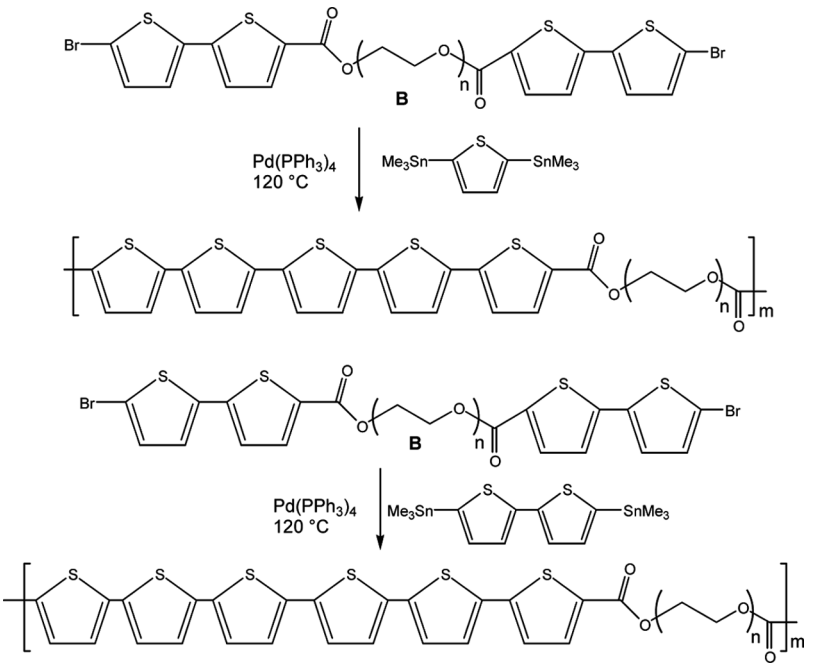

Figure 28. PEO-b-PT via Suzuki cross-coupling [102].

of PANI-b-PEO exhibited helical superstructures when amine-terminated PEO was block extended with PANI prepared by chemical redox polymerization (ammonium persulfate (APS) in 1 M HCl) (Fig. 29). Processing these polymers from diethyl ether/THF lead to the formation of helical superstructures, the result of π-π stacking

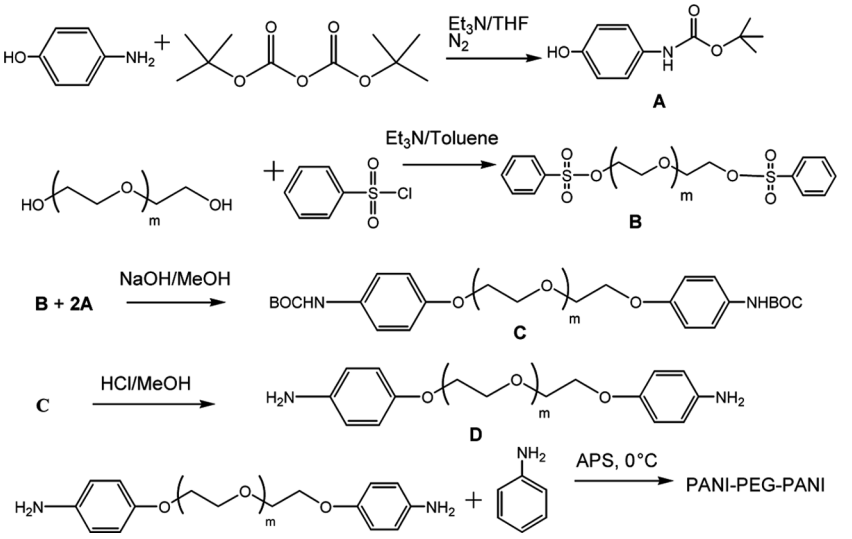

Figure 29. Diblock copolymers of PANI-b-PEO via diamine-functionalized PEO using chemical redox polymerization [104].

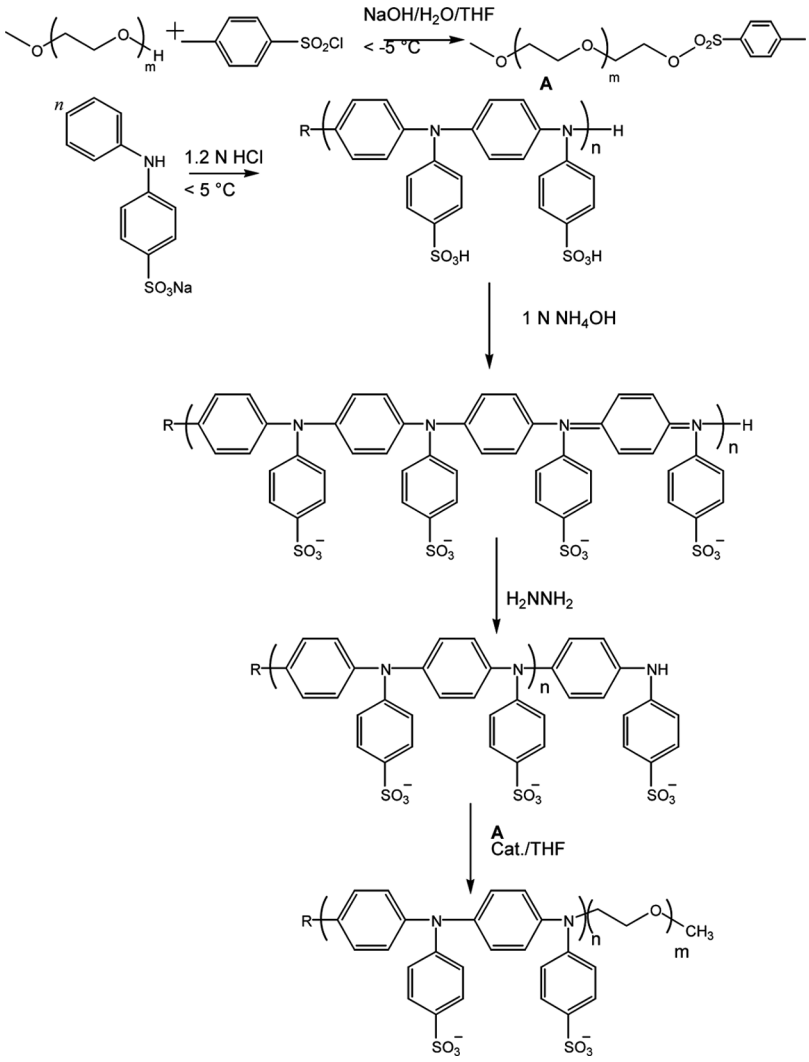

Figure 30. Synthesis of a soluble self-doping block copolymer containing sulfonic-acid modified PANI and PEO [105].

within and between the copolymer chains [104]. A sulfonated polyaniline, poly(sulfonic diphenylaniline) was reacted with a tosyl-chloride functionalized PEO to give water soluble diblock copolymers capable of self-doping via the sulfonic acid groups on the PANI chain (Fig. 30). Conductivities were very low (10^{-3}–10^{-5} S/cm), due to a combination of steric hindrance from the substitution on the PANI nitrogen groups, the withdrawal effect of the sulfonic acid substituent, and a torsional twist from the PEO chain. This effect increases with increasing PEO length, which is why lower conductivities were observed for higher PEO M_n (10^{-3} S/cm for PEO_{350} and 10^{-5} for PEO_{2000}) [105].

PANI and degradable PLA triblock copolymers doped with (10-camphorsulfonic acid) or HCl were prepared from carboxyl-capped aniline pentamers and

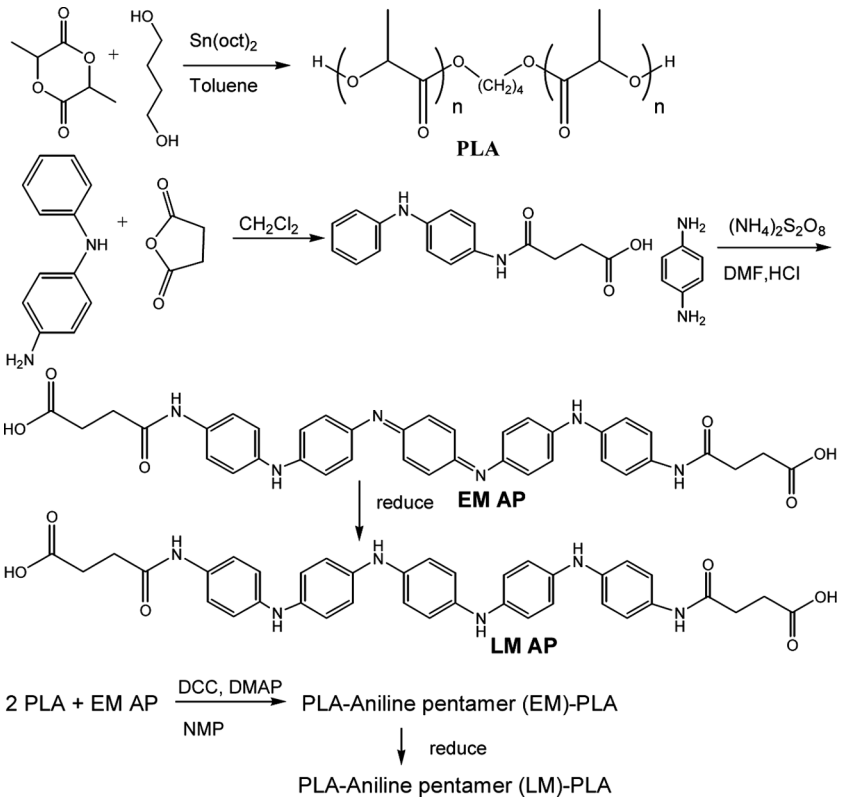

Figure 31. PLA-b-PANI-b-PLA prepared via ROP and chemical redox polymerization [106]. (l) Similar procedures were followed for polyglycolide-based degradable block copolymers (r) [107].

dihydroxyl-capped PLA, resulting in biocompatible and biodegradable materials with low conductivity (10^{-6} S/cm) that exhibit microphase separation [106]. Similar work has been done using aniline pentamers and hydroxyl-capped polyglycolide (PGA) prepared by ROP, giving biodegradable materials with observed conductivities

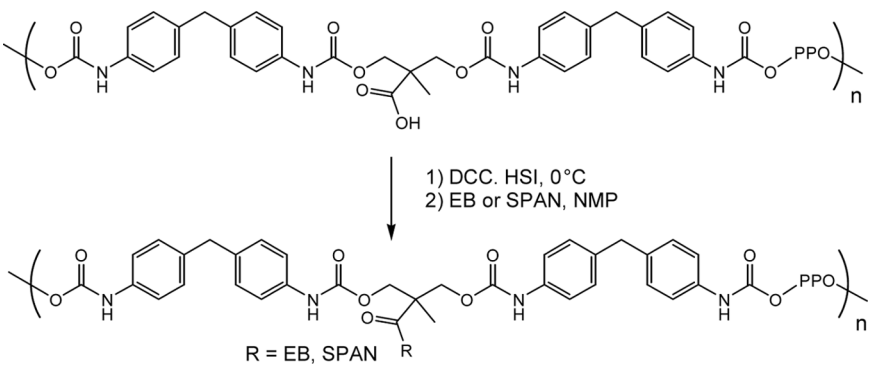

Figure 32. Amidation of polyurethane via $-NH_2$ PANI endgroups [108].

of $\sim 3.9 \times 10^{-5}$ S/cm after doping with HCl [107] (Fig. 31). Block copolymers of PANI and polyurethane (PU) were prepared via amidation of a free carboxyl functionality in the PU backbone with the amine end-group of EB PANI [108] (Fig. 32). Poly(urea-urethane)-b-PANI block copolymers were prepared by mixing PANI oligomers with PU prepolymer and a 1,2-butanediol chain extender until all NCO groups were consumed. These polymers exhibited low conductivities (10^{-2} S/cm – 10^{-5} S/cm) but drastically improved tensile strengths (up to 21 MPa), elongation at break (up to almost 1000%), and Young's moduli (from 50 to 500 MPa) [109].

Graft Copolymers

Conducting Polymer Grafts from Amorphous Backbones

Graft copolymerization is another method for preparing soluble segmented conducting polymer materials; they may contain either a conjugated backbone with amorphous side chains, or am amorphous/crystalline backbone with conjugated side chains. They can be prepared with oligomers or polymers of aniline, pyrrole, and thiophene, prepared by chemical polymerization or electrochemical polymerization (Fig. 33). Early attempts at what are now recognized as graft copolymers were accomplished by Yagci and Toppare [110] (Fig. 34). They prepared an array of thiophene-functionalized macromonomers from ring-opening polymerizations of tetrahydrofuran (THF) (using methyl triflate and triflic anhydride as initiators) [111,112] and octamethylcyclotetrasiloxane (with tetramethylammonium siloxanolate as the initiator and 1,3-bis(3-aminopropyl)-1,1,3,3-tetramethylammoniumdisiloxane as the end-blocking agent) [112–114]. Electrochemical polymerization of pyrrole resulted in what were classified as block copolymers but were more likely graft copolymers containing a mixture of PTHF and PDMS side chains linked through the PPY polymerization [112,115,116]. Pyrrolyl-functionalized RAFT agents such as benzyl 1-pyrrolylcarbodithioate (Fig. 35a) have been used to prepare pyrrolyl end-capped macromonomers of poly(N-isopropylacrylamide) (PNIPAM) that could be incorporated into graft copolymers with the electropolymerization of PPY. This is one of two reported uses of RAFT polymerization to prepare copolymers with conducting materials like PPY and P3HT [117].

Similar behavior was observed for end-capped macromonomers in general, including ϵ-caprolactone [118,119]. PS-b-PTHF (prepared by free radical polymerization from PTHF-functionalized azo initiators) [120], and others, exhibiting

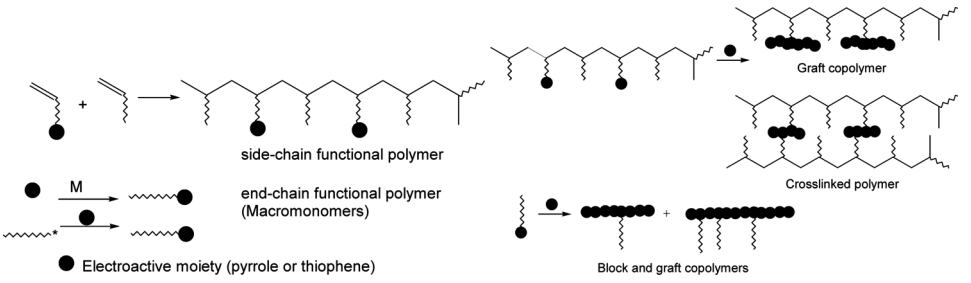

Figure 33. General methods of preparing graft copolymers using heterocycle-functionalized macromonomers [110].

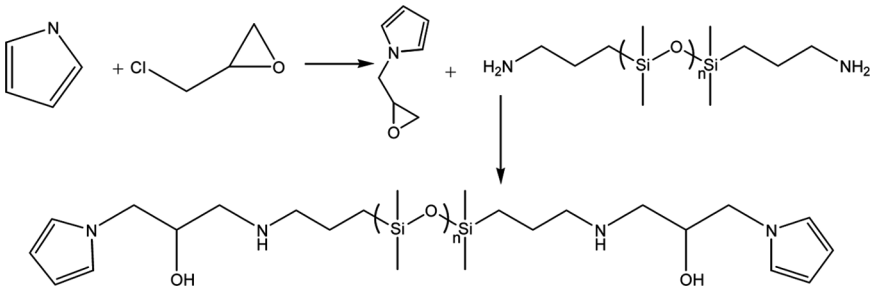

Figure 34. PTHF and PDMS prepared by ring-opening polymerization with pyrrolyl end-caps as precursors to graft copolymers with PPY [60].

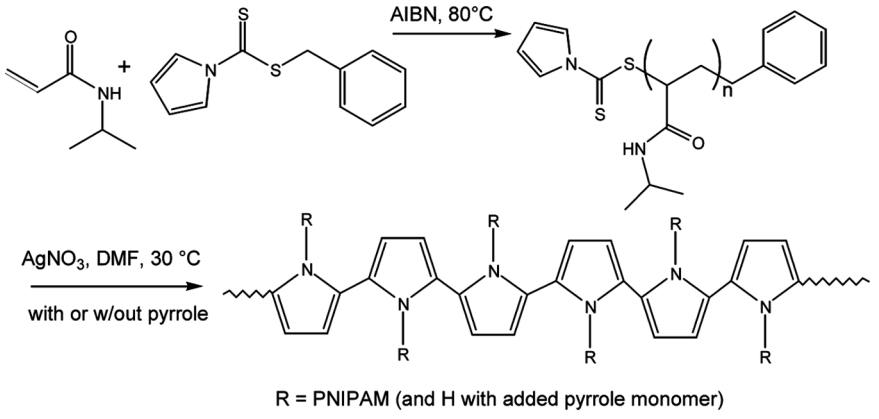

(a)

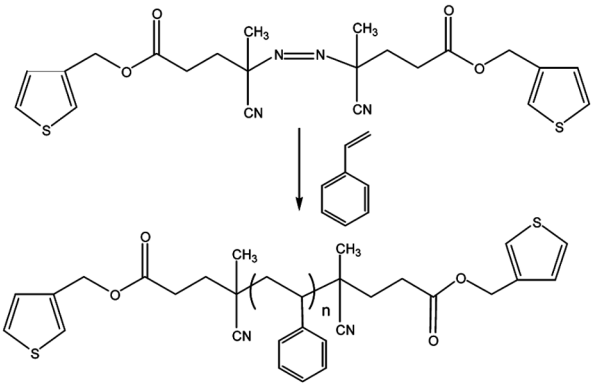

(b)

Figure 35. (a) Pyrrolyl end-capped PNIPAM prepared via RAFT and incorporated into graft copolymers via electropolymerization of pyrrole [117]. (b) (l) Thiophene-functionalized free radical initiator as macroinitiator for conducting graft copolymers [120].

conductivies in a range from 10^{-6} S/cm – 10 S/cm depending on conducting polymer content and the method of polymerization (electrochemical, chemical, etc) [120]. Polyglycidol–block-poly(L,L-lactide) was modified by 3-(pyrrol-1-yl)-propanoic acid at both the end groups and on the glycidol pendent moieties and micellized, using a solvent-displacement procedure to form nanoparticles. During electrochemical polymerization in pyrrole these functionalized biodegradable nanoparticles were grafted into the polymer film through the terminal and pendent pyrrole functionalities on the polymer chain [121].

Functionalizing poly(2-chloroethylvinyl ether) with a pyrrole group in place of the chlorine moiety offered a mechanism for obtaining conducing polymer grafts via chemical or electrochemical polymerization through the pyrrole pendent group, resulting in smooth films that exhibit no polypyrrole loss after washing, likely due to the grafted/crosslinked nature of the polymer film [122] (Fig. 37). Similar work was done with a thiophenized pendent group, 3-methylthionyl methacrylate, which was polymerized using azobis(isobutyronitrile) (AIBN) as the radical initiator for free radical polymerization. The thiophene side groups were then polymerized through polypyrrole and polythiophene via electrochemical polymerization, chemical polymerization with $FeCl_3$ and galvanostatic polymerization in order to incite self-polymerization among the thiophene side chains. Polypyrrole graft copolymers exhibited conductivities between 0.9 and 3 S/cm, while polythiophene grafts had conductivities on the order of 10^{-3} S/cm. All graft copolymers exhibited similar morphologies, smooth films on the electrode side and cauliflower-shapes in solution [123] (Fig. 38). N-(4-(3-Thienylmethylene)oxycarbonylphenyl)maleimide (MBThi) was copolymerized with styrene by photoinitiated polymerization to give random copolymers that could also be grafted through the side thiophene groups (Fig. 39) to produce conducting polymer films of either PPY or PT with conductivities of 0.1–0.7 S/cm [124].

Similar work was done to functionalize a block copolymer of poly(*p*-chloromethylstyrene) (PCMS) and poly(methyl methacrylate) (PMMA) with a pyrrole moiety on the styrene group. This pyrrole group was then polymerized with

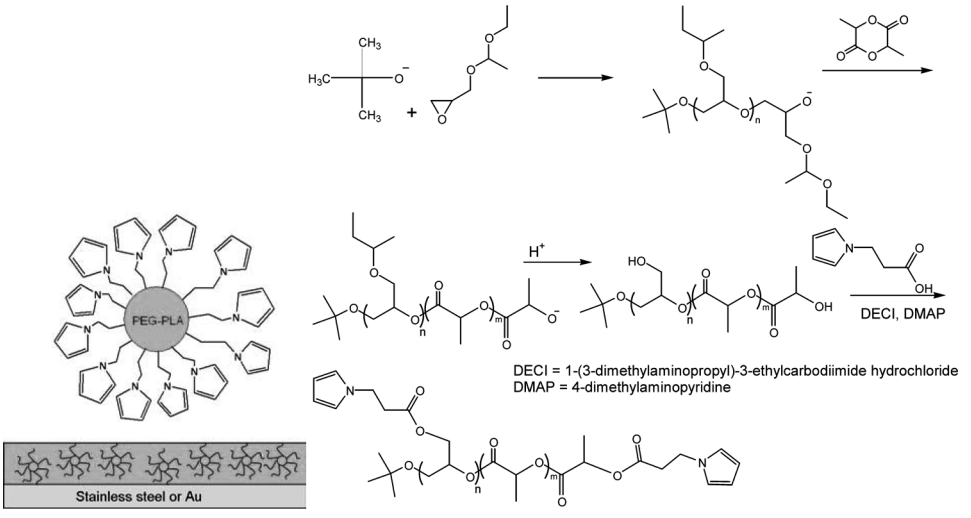

Figure 36. Polylactide-based nanoparticles with grafted polypyrrole [121].

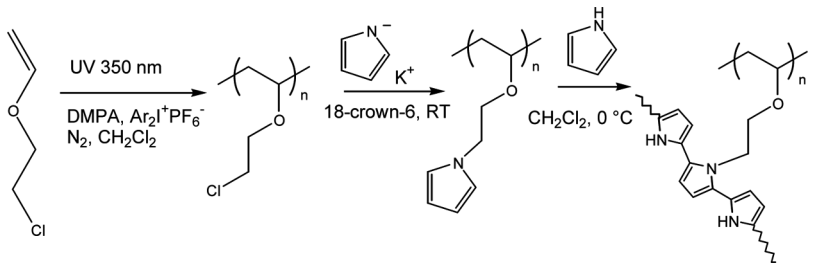

Figure 37. Preparation of graft copolymers from poly(2-chloroethylvinylether) functionalized with pyrrole [122].

pyrrole in solution via electrochemical polymerization that, from cyclic voltammetry measurements, occurred preferentially to the polymerization of pyrrole in solution, resulting in favorable graft copolymer formation. Conductivities were higher for the graft copolymers than for simple mixed composites of the block copolymer and PPY ($\sim 10^{-1}$ S/cm vs 10^{-3} S/cm) [125]. Using a copolymer of styrenesulfonic acid and CMS, followed by reaction with a potassium pyrrole salt, the pyrrole unit is covalently attached to the CMS group in place of the chlorine (Fig. 40). This pyrrole can then be polymerized via electrochemical or chemical methods (using $FeCl_3$ or APS) to produce graft copolymers with conductivities of 4.8×10^{-1} S/cm with 36 wt% PPY [126].

Amorphous Grafts from Conducting Polymer Backbone

Conducting polymers have also been used as the backbone to provide grafting sites for more soluble amorphous polymers like PMMA [127] and PS [128] as well as the

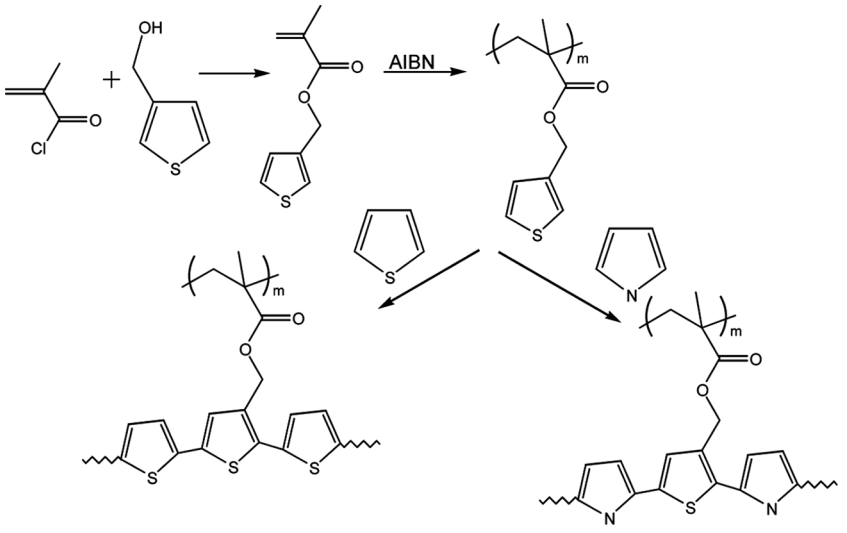

Figure 38. Thiophene-functionalized methacrylate polymerized by free radical polymerization as conducting graft copolymer precursor [123].

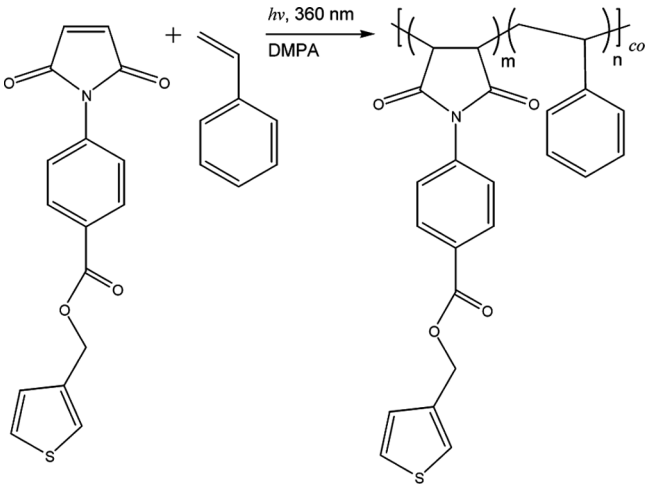

Figure 39. MBThi-containing random copolymers as precursors to conducting graft copolymers through the thiophene moiety [124].

electron donor quinoline (with vinyl functionality) [129] (Fig. 41). The procedure for these involves the co-synthesis of PT or P3HT with either a protected hydroxyl-functionalized thiophene (using TMS) or a bromine-functionalized thiophene that could later be substituted with the desired hydroxyl functionality. The hydroxyl-functionalized side chain was then reacted with 2-bromopropionyl bromide or chloride to form the ATRP initiating site, which was then block extended using classic ATRP techniques to form grafted side chains of the desired amorphous polymer. This type of grafting led to 20-fold improvement in the fluorescence of the polythiophene in these materials because the amorphous chains prevent π-stacking and aggregation while also preserving solution conformation in the solid state.

Polythiophene-*graft*-(styrene-*g*-C_{60}) copolymers were also prepared to take advantage of the improved optical properties of these grafted materials [130]. Poly(3-hexylthiophene) was first functionalized with bromine, followed by reaction with a boronic-ester-modified TEMPO-based initiator (Fig. 42). This polymer was then extended with a mixture of styrene and CMS (3:1 and 5:1 feed ratios) and the C_{60} functionality was attached by atom transfer radical addition (ATRA), resulting in some crosslinking of the material. Photoluminescence spectra demonstrated

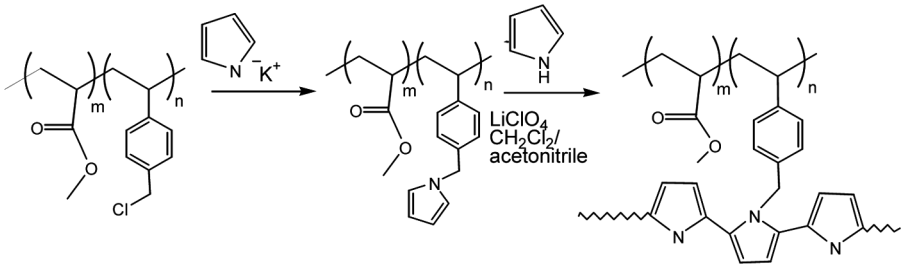

Figure 40. *p*-Chloromethylstyrene-containing block copolymers as precursors for conducting graft copolymers [126].

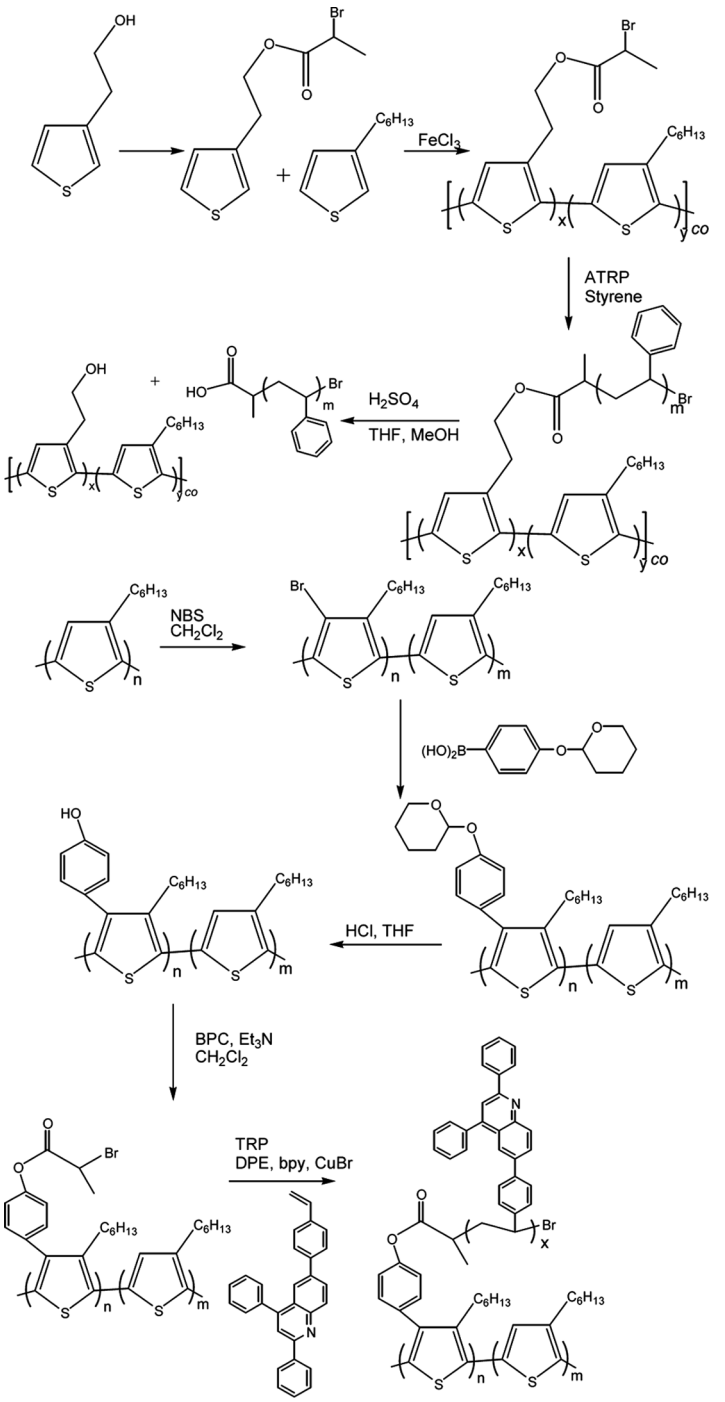

Figure 41. Grafting from P3HT backbone via functionalization with ATRP initiators [128,129].

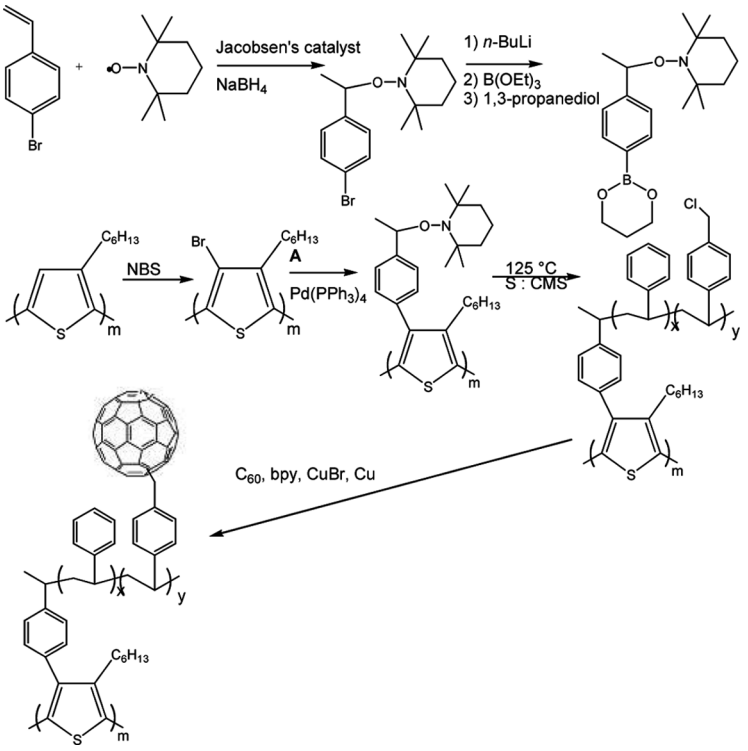

Figure 42. Preparation of grafted P3HT copolymer and functionalization with C_{60} [130].

complete quenching in the C_{60}-functionalized polymer, while a blend of block copolymer and 'free' C_{60} exhibited only moderate quenching. This is attributed to the small distance between the C_{60} moiety and the conducting polymer provided by covalent linkages and block copolymer self-organization. The spacing for the C_{60}-functionalized copolymer is much less than that for the 'pure' block copolymer, thus providing the more efficient D-A transition demonstrated by total fluorescence quenching.

Some grafting may also be due to non-covalent interactions rather than chemical bonds. For instance, the surface of a PANI film can be 'grafted' with PPO-PEO-PPO (pluronic) chains by the two liquid entrapment techniques. This involves partial solubilization of the PANI film in a good solvent (N-methylpyrrolidone, or NMP) in the presence of the pluronic polymer to allow entanglement between the dissolved PANI and the pluronic polymer. This is followed by submersion in water, which functions as a poor solvent and traps the PANI and pluronic in their entangled state, resulting in a PANI surface modified by amphiphilic polymer chains that cannot be removed (Fig. 43) [131]. This absorption lowers the conductivity a modest amount, but increases the biocompatibility of the PANI film, which is useful in most biological applications. A different kind of grafting by noncovalent interactions involves the use of acidic functionalities to complex with the nitrogen groups in PANI via acid-base interactions. A PANI nanorod, for instance, can be rendered soluble by complexing a poly(acrylic acid)-b-poly(ethylene oxide) (PAA-b-PEO) to the nanorod surface through the ionic interaction between the deprotonated acid group and the

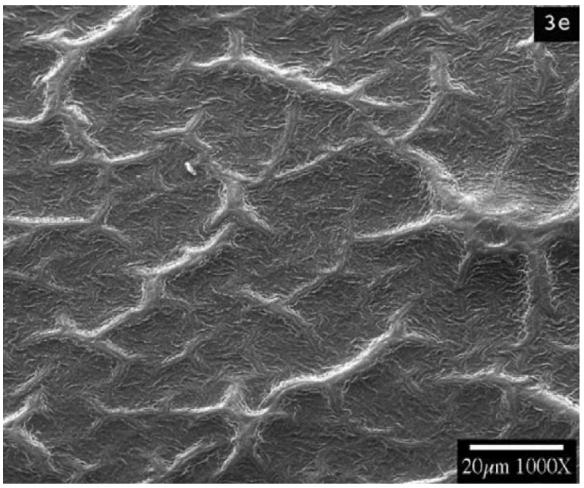

Figure 43. PANI film with noncovalently-grafted PEO-b-PPO-b-PEO on the surface [131].

protonated nitrogens in the PANI backbone. This, combined with the hydrophilicity of PEO, results in water-dispersible PANI nanostructures [132]. Silica nanoparticles have also been grafted, first with a layer of 4-vinylaniline and UV-induced coupling to the Si-H surface. Subsequent aniline polymerization occurred via chemical oxidative polymerization using APS and 0.5 M aniline monomer. Sulfonyl chloride groups were introduced to the PANI backbone via a reaction with chlorosulfonic acid. Styrenesulfonate monomer was then polymerized using ATRP with CuCl/bipy as the catalyst, [133] and the resultant material was either submerged in 1 M HCl to give styrenesulfonic acid, or the PSS chains were block extended with poly((ethylene glycol)monomethacrylate) (PEGMA) using CuCl, $CuCl_2$ and bipyridine (Fig. 44). This method is a fairly simple way to prepare self-dopable grafted nano-objects [133].

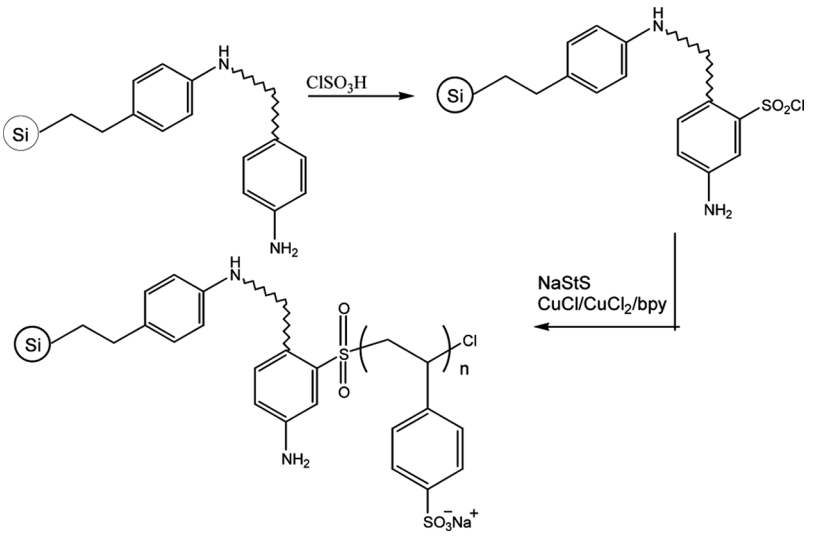

Figure 44. Silica particles grafted with PANI and polystyrenesulfonate [133].

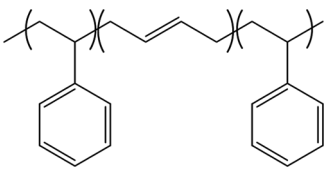

Figure 45. Styrene-butadiene-styrene (SBS) block copolymer. PANI exhibits a weak preference for the PS domains of this block copolymer.

Block and Brush Copolymers as Templates for Conducting Nanomaterials

Linear Block Copolymer Templating via Affinity

One of the simplest methods for templating conducting polymers involves the use of a soft block copolymer template with one segment/phase that exhibits a preference for the conducting polymer. In the case of styrene-butadiene-styrene (SBS) (Fig. 45), aniline exhibits a weak preference for the styrene domains, giving those areas a higher PANI content [134]. Using *in situ* polymerization of aniline via either emulsion or inverse emulsion pathways in the presence of SBS results in the preparation of materials with conductivities on the order of several S/cm, much higher than the conductivities formed from bulk mechanical mixing of PANI and SBS [134–136]. This higher conductivity is accompanied by a significantly lower percolation threshold, due in part to the presence of increased PANI amounts in the styrene phase, and in part due to the fibrillar morphology adopted by PANI prepared *in situ*, while pre-prepared PANI is incorporated as large particle agglomerates [136]. PANI also interrupted the physical crosslinks of PS with itself, resulting in lower tensile strengths and elongation at break with increasing PANI content. In addition to the method of preparing the blended template, processing of the PANI-containing material is also an important parameter [137]. Processing the templated copolymer by melt processing vs solution processing changes the percolation threshold from 10% to 7%, while secondary doping with *m*-cresol lowers the percolation threshold of solution-processed materials to 3% [137,138].

Partially sulfonated polystyrene-*b*-poly(ethylene-*ran*-butylene)-*b*-polystyrene copolymers (Fig. 46) (SEBS) were also used as templates for PANI doped with DBSA. The conductivities in these materials were comparable to those from non-sulfonated SBS, and the percolation threshold, without *in situ* polymerization of PANI, was <3 wt% for the pure SEBS and <2 wt% for sulfonated SEBS, as the sulfonate groups can function as counterions for the positive charges in the doped

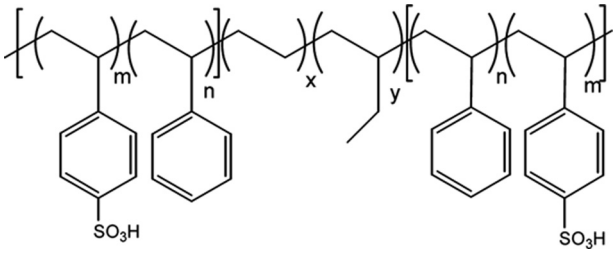

Figure 46. Chemical structure of sulfonated SEBS which can function as a PANI template [139].

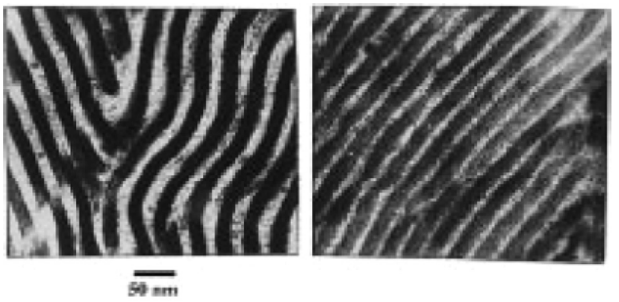

Figure 47. TEM images of (a) sulfonated poly(styrene-*b*-(ethylene-*alt*-propylene)) (SEP) diblock copolymer (b) SEP with 4.8 wt% PPY [140].

polymer, and thus the PANI content of the styrene phase will increase [139]. Similar work was done with a poly(styrene-*b*-(ethylene-*alt*-propylene)) (SEP) diblock copolymer whose styrene segment had been sulfonated in order to provide lamellar microdomains that were more prone to swelling by a solution of water, pyrrole monomer, and oxidant prior to polymerization (Fig. 47). This swelling resulted in preferential formation of PPY in the sulfonated domains of the SEP block copolymers, giving templated polymer materials with conductivities of $10^{-3}-10^{-1}$ S/cm parallel to the surface at 5 wt% and 11 wt% PPY respectively [140].

Block copolymers of polystyrene and 2- or 4-vinylpyridine are also frequently used as a method for templating conducting polymer materials, often as a means of obtaining spherical PPY from as-cast polymers that either self-assemble into spherical P2VP domains in a PS matrix [141] (Figs. 48, 49) or as block copolymer micelles cast on surfaces [142]. The P2VP domains may also be used as sites for simultaneous conducting polymer polymerization and gold nanoparticle deposition (Fig. 50), creating hybrid films with a variety of potential uses [143,144]. Films of PS-P2VP with lamellar morphologies were used as preferential templates for the preparation of PPY-containing materials with high anisotropic conductivity [145]. This behavior was also observed for PS-b-P*n*BA block copolymers with lamellar microdomains (Fig. 51); *in situ* polymerization of pyrrole resulted in localization of

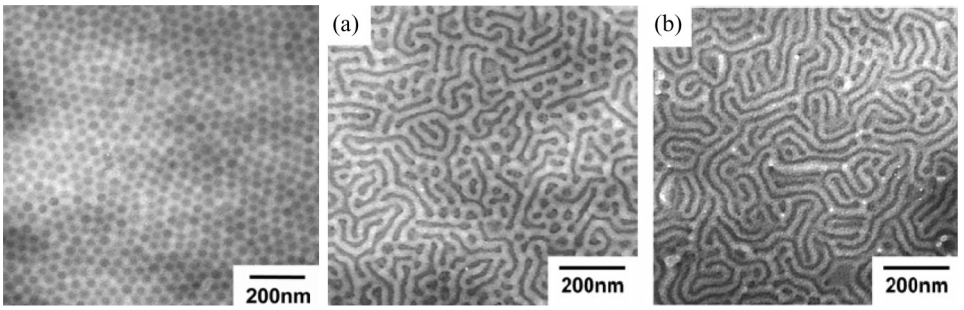

Figure 48. PS-P2VP (with $FeCl_3$ in P2VP domains) with no PPY polymerization, a) after 20 minutes exposure to pyrrole vapor b) after 3 hours exposure to pyrrole vapor [141].

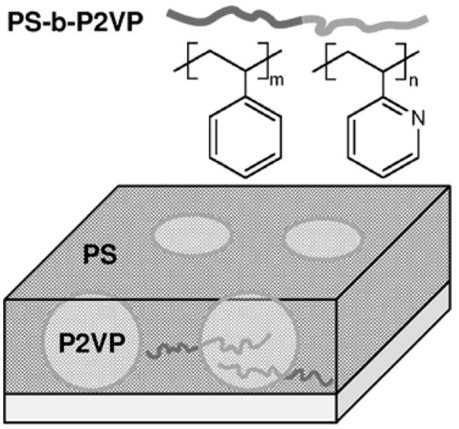

Figure 49. Schematic of PS-b-P2VP nanostructured film.

the PPY in the P*n*BA regions of the film, with a percolation threshold of 2 wt% PPY and conductivities as high as 10^{-1} S/cm parallel to the domain orientation [146].

Those same interactions were utilized to create spherical nanostructured conducting materials that were easily produced from both as-cast films with 1,4-diiodobutane-crosslinked P2VP microdomains and via solution polymerization

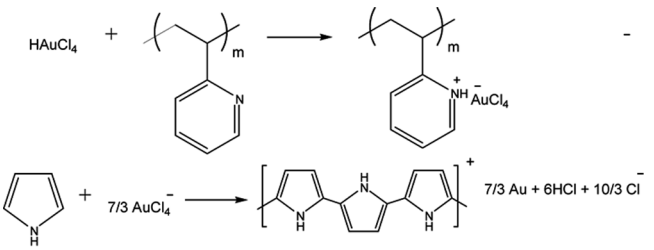

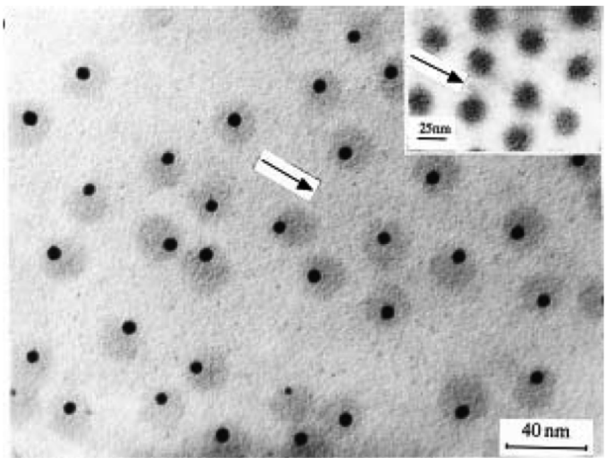

Figure 50. PPY templated on gold nanoparticles inside PS-b-P2VP block copolymer matrices [91].

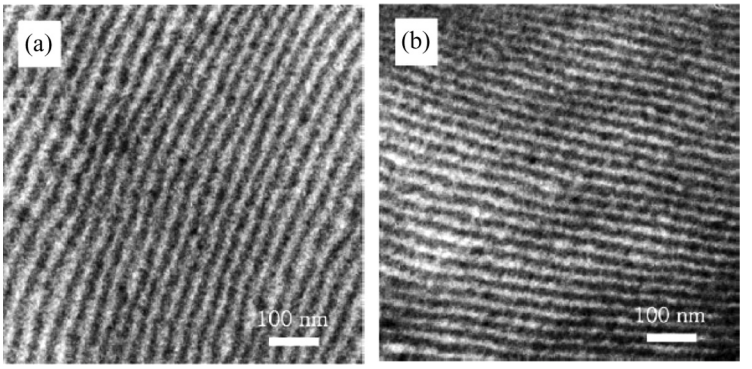

Figure 51. (a) PS-b-P*n*BMA with 50 wt% PS, M_n 72,000 g/mol, and PDI 1.03. (b) PS-b-PnBMA with 15 wt% PPY [146].

of micelles with crosslinked P2VP cores. Polypyrrole was directly formed in the P2VP domains of the block copolymer due to the oxidant Cu^{2+} (from $CuCl_2$) bonded to the nitrogen moieties on the pyridine rings. Vapor phase polymerization resulted in the formation of PS-shell-PPY-core micelles; these materials exhibited very low conductivities (10^{-13} S/cm) due to the isolation of the PPY microspheres within the insulating PS matrix [147] (Fig. 52). A similar method with Cu^{2+} bound to pyridine rings was used to prepare PPY within the core of a poly(α-methylstyrene)-*b*-poly(2-vinylpyridine) (PMS-b-P2VP) brush prepared by free radical polymerization of a PMS-b-P2VP macromonomer. This resulted in formation of PPY nanowires encapsulated within an insulating matrix, though the continuous nature of the encapsulated nanowires was not determined [148]. Self-assembled arrays of crosslinked PS microspheres and asymmetric PS-b-P2VP were cast from formic acid in which PANI doped with phenolsulfonate had also been dissolved (Fig. 53). Due to the low volume fraction of P2VP PS and the affinity of PANI for the pyridine rings, PANI:PSA was finely dispersed in the P2VP domains. The percolation threshold of the PANI in this material was thus significantly lower (1.1%) than previously observed due to the double percolation from P2VP to PANI [149].

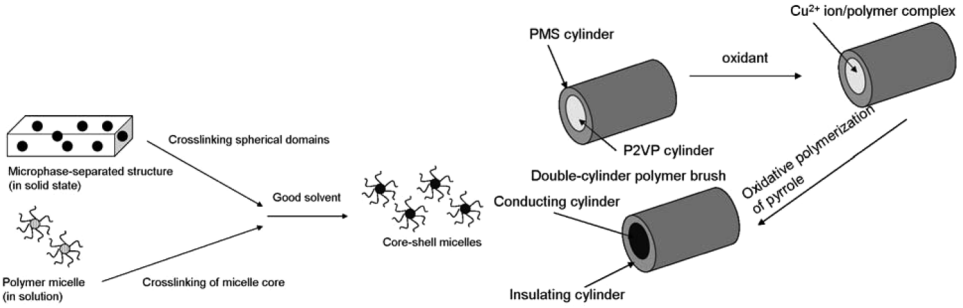

Figure 52. (l) Spherical PPY nanostructures from porous membranes or polymer micelles using Cu^{2+} bound to P2VP domains. (147) (r) PPY from cylindrical brushes prepared by free-radical polymerization with P2VP domains coupled with Cu^{2+} [148].

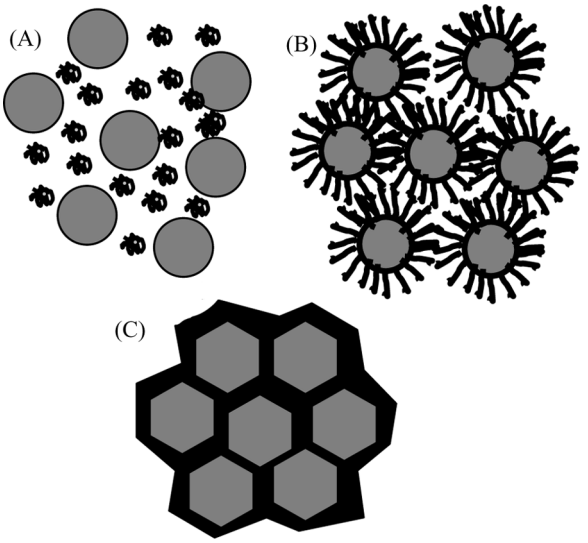

Figure 53. PANI templated in the interstitial spaces between PS microspheres with PS-P2VP functioning as templating agent [149]. (A) PS microspheres (gray) with free PS-PZVP block copolymer (black) in solution. (B) Doped PANI templated by P2VP segments of the PS-P2VP block copolymer. (C) After drying, PANI is concentrated in the interstitial space with the P2VP blocks.

Block copolymers of 2-acrylamido-2-methyl-1-propanesulfonic acid (AMPSA) and methyl or *n*-butyl acrylate [150] were used as templates for nanostructured PANI when dissolved in dichloroacetic acid (DCAA) [36]. In these materials the sulfonic acid groups on the AMPSA block functioned as proton-donating dopants for PANI, and subsequently served as counterions for the positively charged PANI backbone. This resulted in the selective presence of PANI in the hard acidic domains, allowing for control of the PANI morphology by manipulating the molecular weight and composition of the templating block copolymers. Conductivities in these systems reached values as high as 30 S/cm with templates of 15–30 wt% AMPSA, and percolation thresholds were at $\sim$10 wt% PANI. The use of low T_g materials as the hydrophobic blocks also resulted in improved mechanical properties, reducing the brittleness of pure PANI and creating materials that could reach 20–50% elongation under stress, with breaking strains of up to 4 MPa [151,152].

Block Copolymers as Soft Porous Membrane Templates

With PS-P4VP, the spherical hexagonally-arranged P4VP domains in the as-cast films can be swollen with pyrrole and polymerized with pre-loaded $FeCl_3$ catalysts to prepare extended cylindrical structures. These structures can undergo rearrangement to spherical cavities when dipped into a P4VP-selective solvent such as ethanol [141]. Similar cavitation can be accomplished using PS-P2VP block copolymers with spherical P2VP domains; treatment of the as-cast polymer micelles with acetic acid resulted in cavities that exposed the surface of the substrate. Subsequent electrochemical polymerization of PANI resulted in entwined PANI nanofibers that exhibited the same number of nucleation sites and uniform fiber diameters regardless of

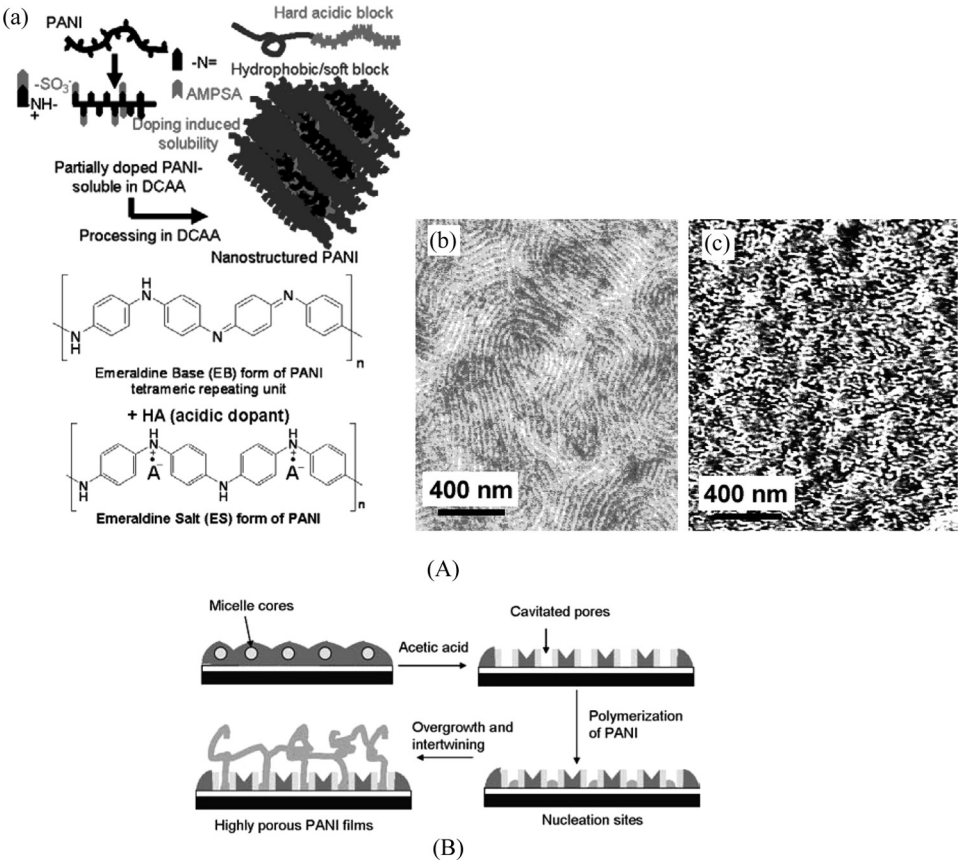

Figure 54. (A) (a) Polyaniline complexation with functionalized acidic block copolymers. The imine nitrogens on the emeraldine base (EB) form are protonated by acidic protons to give a positively charged emeraldine salt (ES). (b) Phase contrast TMAFM image of $4EB_{11.5}/(AMPSA)_{23}$-*b*-$(MA)_{290}$ (c) Phase contrast TMAFM image of $PANI(AMPSA)_1)_{2.3}/(AMPSA)_{23}$-*b*-$(MA)_{290}$. (B) PANI nanofibers formed in the pores of PS-P2VP films treated with acetic acid to encourage cavitation. Similar porous templates can be formed after treatment with other solvents, such as ethanol, and may also be used with other conducting polymers such as PPY. Denser arrays of pores will result in nanorods over nanofibers due to spatial constraints during synthesis [153].

the current density during polymerization, a result of the initial stages in which PANI nanoparticles are formed in the surface cavities [153] (Fig. 54).

PS-P2VP is not the only polymer that has been used as a soft template for the preparation of conducting polymer nanostructures. Polystyrene-*b*-poly(acrylic acid) (PS-b-PAA) (from PS-b-P*t*BA block copolymers prepared by ATRP), which forms a hexagonal lattice after treatment with CS_2 in water vapor and subsequent drying, was used as a porous template for the electrochemical polymerization of PANI on the exposed surface. Uniform areas 3–7 μm in diameter were covered with PANI, corresponding to the template pore size [154,155]. PS-b-PMMA block copolymers have also been used as porous templates; swelling of the PS-b-PMMA with homopolymer PMMA prior to film casting resulted in PMMA nanocylinders that were removed via extraction with acetic acid, a PMMA-selective solvent. Polypyrrole

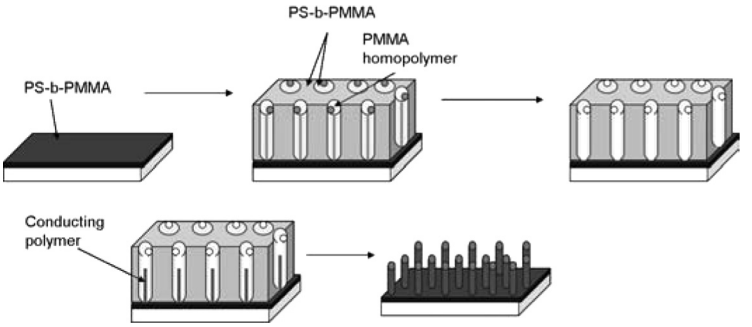

Figure 55. Conducting polymer assembled in the pores of a PMMA-b-PS membrane swollen with PMMA homopolymer [156].

was then electropolymerized from the ITO-coated surface to form an array of dense, well-aligned polypyrrole nanorods that were easily separated from the PS-b-PMMA template by washing with toluene. This method can be extended to P3HT and PEDOT as well, on a wide variety of flexible conducting surfaces [156] (Fig. 55). A similar method was also used to prepare PPY nanomushrooms on gold electrodes to increase the available surface area [157] (Fig. 56). Block copolymers materials in the bulk, such as poly(cyclohexylethylene)-*b*-polylactide (PCHE-b-PLA) or PS-b-PLA, which contain a degradable block, can also be made into porous templates [158–160]. Impregnation with the $FeCl_3$ catalyst and subsequent vapor phase polymerization of the pyrrole monomer result in PPY nanowires of controllable dimensions based on the pore sizes in the block copolymer template [161] (Fig. 57). Surface-tethered PMMA brushes grown by ATRP can also function as negative masks for the polymerization of conducting polymers like PPY with appropriate photopatterning, resulting in well-controlled PPY growth [162] (Fig. 58).

Block Copolymer Micelles as Nano-Object Templates

Block copolymer templates can also aid in the formation of discrete nano-objects. Self-organization of PS-b-PAA in aqueous solution results in the formation of

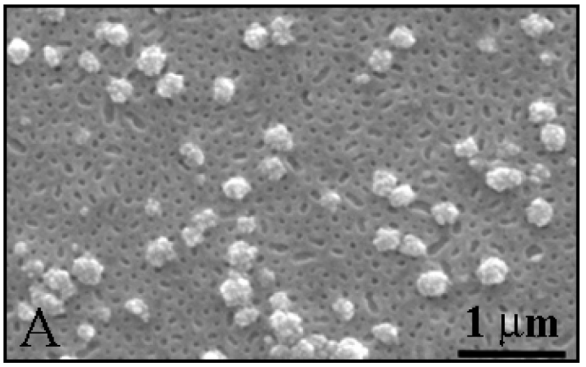

Figure 56. PPY nanomushrooms grown by electrodeposition from a porous PMMA-b-PS template after UV etching of PMMA domains [157].

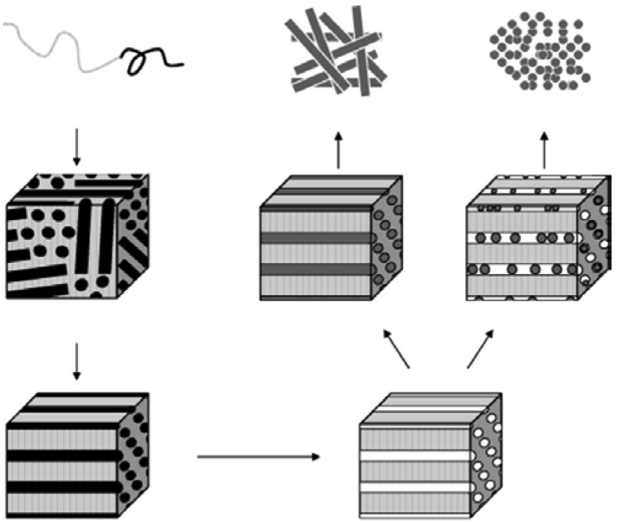

Figure 57. Conducting polymers (shaded rods) assembled in the porous core of self-assembled polymeric materials with degradable polylactide segments [161].

micelles that will complex with pyrrole through the acid groups and allow templated polymerization of conducting nanoobjects via oxidation of pyrrole monomer with APS [154] (Fig. 59). Length of the hydrophilic PAA block was the primary controller of the micelle shape; increasing the PAA content resulted in transitions from vesicles to rods to spheres. PAA also functions as the dopant, leaving the decomposition temperature of the hybrid particles somewhat lower than expected for pure polypyrrole. Similar work was done with block copolymers of 2-acrylamido-2-methyl-N-propanesulfonic acid (AMPSA) and poly(methyl acrylate) prepared by ATRP, resulting in near monodisperse preparations of water-soluble doped PANI nanoparticles [163] (Fig. 60). Block copolymer micelles of PS-b-PEO swell in water when aniline monomer is added, because polystyrene is soluble in aniline. Due to the insolubility of PS in water, the oxidant and anilinium monomer for polymerization are not present in the PS core, instead polymerization occurs at the core-shell interface, resulting in the formation of a PANI shell around the frozen PS core. Use of equimolar amounts of HCl as the dopant also functions to stabilize the colloidal

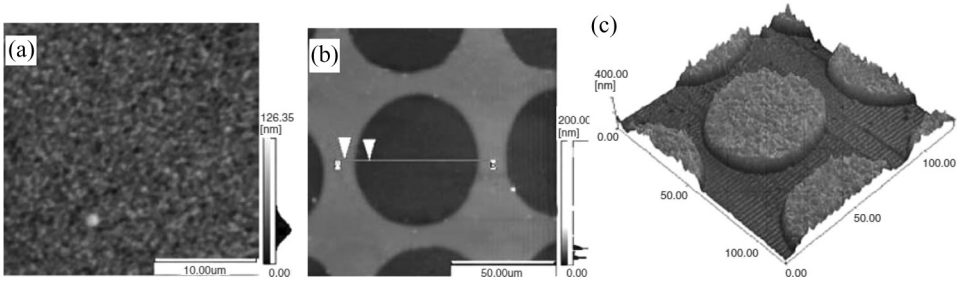

Figure 58. (a) PMMA brush from surface-initiated ATRP (b) PMMA brush patterned via UV exposure (c) PPY nanoarrays grown from the deprotected surface [162].

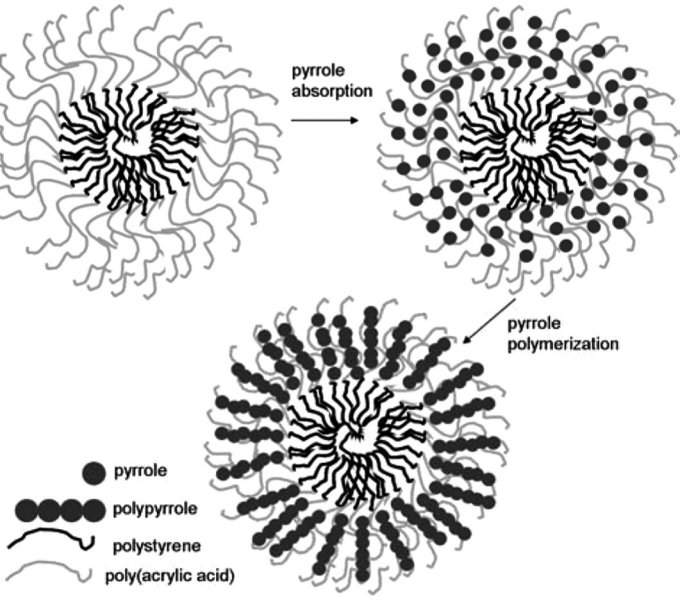

Figure 59. PPY templated on PS-b-PAA block copolymer micelles with PAA as dopant [154].

particles, particularly if the acid is added to the system last [164]: PMMA-b-PAA block copolymers have also been used in the preparation of polypyrrole-coated nanoparticles in much the same manner [165]. PS-P2VP micelles have also been used as templates for the self-assembly of P3HT and quantum dot nanoarrays for light harvesting [166] (Fig. 61).

Our group used triblock copolymers containing a central hydrophobic acrylate block and exterior AMPSA blocks have also been used as micellar templates for the *in situ* polymerization of PANI and PPY [151]. Micelle sizes were approximately 70 nm prior to addition of pyrrole or aniline monomer, while the subsequent

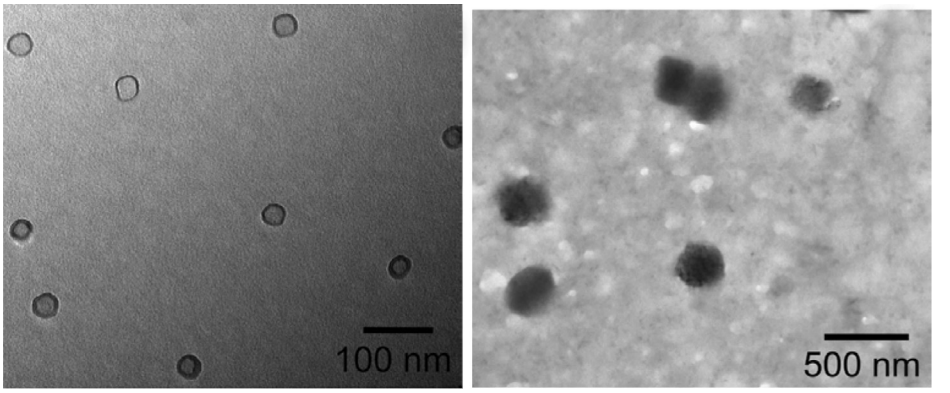

Figure 60. (a) PMA-b-PAMPSA micelles with a clear core-corona arrangement (b) PANI templated on the PMA-b-PAMPSA micelles in deionized water [163].

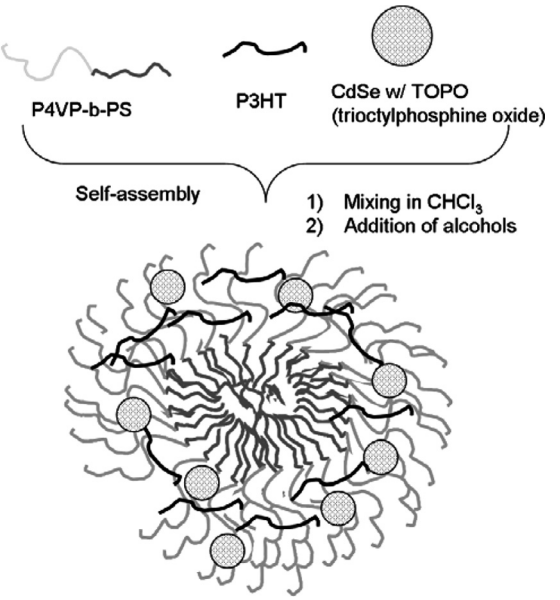

Figure 61. P3HT and quantum dots templated on PS-b-P2VP micelles [166].

conducting nano-objects post-polymerization exhibited sizes of up to 500 nm as a result of crosslinking and aggregation during the oxidative polymerization with ammonium persulfate (APS) (Fig. 62). These conducting particles were spherical, as determined with AFM measurements (Fig. 62b), and PPY particles exhibited conductivites up to 0.25 S/cm when processed from N-methylpyrrolidone. Post-process doping using bis(2-ethylhexyl sulfosuccinate) (AOT) and monomeric AMPSA resulted in increased conductivities – up to 0.7 S/cm. PANI-based nanostructures exhibited lower conductivities, a result of significant amounts of undoped EB PANI in the micelles as observed by UV-Vis spectroscopy. Dialysis of these suspensions vs. 0.1 M HCl resulted in improved conductivities on the order of 10^{-1} S/cm.

Conducting Nanostructured Carbon Prepared by Block Copolymer Templates

Templating Block Copolymers with Added Low MW Carbon Precursors

Similar methods have also been used for the preparation of nanostructured carbon materials, particularly those involving the use of porous membranes as templates for carbon nanrods or mesoporous carbons and the use of block copolymer micelles as controllable templates for multiple nanostructures. The carbon derived from such organic precursors is not perfectly graphitic, but the content of the graphitic clusters can be increased based on processing conditions, including annealing and pyrolysis temperatures.

Polymer membranes used as templates in the case of carbon nanotubes are often polystyrene-*b*-poly(methyl methacrylate) (PS-*b*-PMMA) block copolymers (~30 wt% PMMA) that are cast as thin films and annealed to form phase-separated structures with fairly uniform cylindrical PMMA domains perpendicular to the

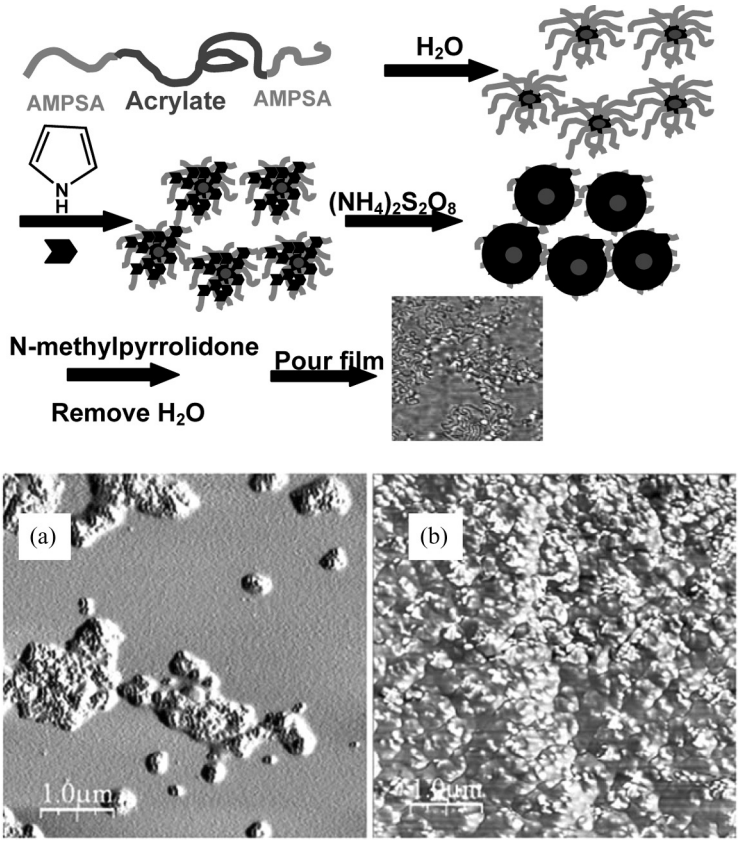

Figure 62. Triblock copolmers containing AMPSA and ethyl or *n*-butyl acrylate as templates for *in situ* preparation of PANI and PPY (a) AFM images of $AMPSA_{30}BA_{156}AMPSA_{30}$ with (a) 5 wt% polypyrrole and (b) 25 wt% polypyrrole cast from 0.5 mg/mL solutions in DMF onto silica substrates [151].

substrate. These PMMA domains are removed by UV irradiation, and iron are deposited in the pores prior to removal of the PS domain by washing with a good solvent like toluene (Fig. 63). Carbon vapor deposition on the patterned substrate allows for the preparation of densely packed carbon nanotube arrays with uniform sizes constrained by the size of the initial PMMA-based pores [167]. The size distributions in the case of polymer film-patterned nanoarrays is significantly narrower (with smaller nanotube diameters) than from catalyst particles freely deposited on a bare substrate, and also allows for significantly controlled patterning of the nanotube films on the microscale [168].

Hard templates are also effective for the production of organically-derived carbon nanotubes as well, particularly anodic aluminum oxide membranes. Combining these membranes with block copolymers such as polystyrene-b-poly(4-vinylpyridine) (PS-b-P4VP), which can easily infiltrate the pores in the AAO, provides a second level of structural control for the formation of porous carbon nanorods and nanotubes (Fig. 64). The P4VP block of the copolymer exhibits affinity for carbohydrates such as raffinose, glucose, and turanose, which also function as

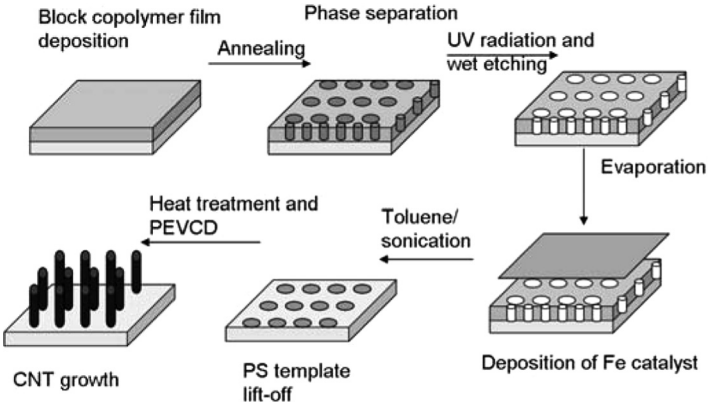

Figure 63. Porous PS-b-PMMA membranes templating the growth of carbon nanotubes [167,168].

carbon precursors. Adding these carbohydrates to AAO/PS-P2VP composites and carbonizing them above 460°C produces 200 nm-long nanotubes with mesoporous of ~16 nm. When the precursor polymers are annealed under benzene/DMF at 80°C, they exhibit more uniform mesopore sizes and distributions in the final carbon materials [169]. Mesoporous thin films and nanospheres can be prepared from the same PS-P4VP block copolymers either from thin-film casting onto glass, or silica substrates, or from an aerosol process [170]. Subsequent addition of the carbohydrate-based carbon precursor and pyrolysis at elevated temperature (>450°C) resulted in the formation of porous carbons with high surface areas of $530\,m^2\,g^{-1}$, where preliminary cyclic voltammograms indicate moderate specific capacitance

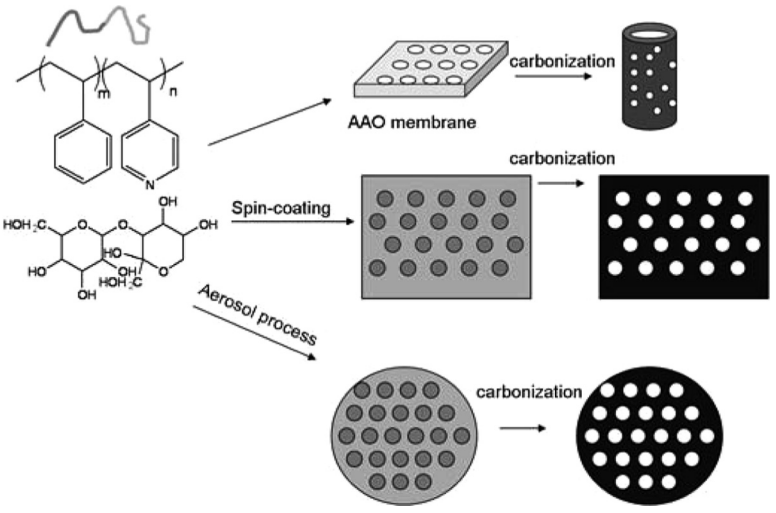

Figure 64. PS-b-P4VP as templates to control the nanostructure of carbohydrate-based carbon precursors. AAO membranes result in porous nanotubes, while spin-coating gives porous thin films and aerogel processes result in the formation of porous carbon nanospheres [169,170].

(81 F/g) that may make these carbons suitable for components in capacitors or lithium ion batteries. Hollow porous carbon nanospheres were prepared from PEO-b-PS block copolymers [170]. Using PS-P4VP as the template with phenolic resin as the carbon precursor allows for the preparation of carbon nanoflakes or nanosheets, as the precursor material takes on a lamellar structure with addition of the resin due to hydrogen bonding between the phenolic residues and the nitrogen in P4VP [171].

In addition to thin films and aerogels, mesoporous carbons have also been prepared from micellar suspensions. Triblock copolymers poly(ethylene oxide)-b-poly(propylene oxide)-b-poly(ethylene oxide) (PEO-b-PPO-b-PEO) have frequently been used in the preparation of mesoporous silica, while the inverse triblock copolymer PPO-b-PEO-b-PPO has often been used for the preparation of mesoporous carbon derived from resorcinols. The phenolic resins form hydrogen bond with the PEO segments, resulting in specific formation of carbon in those domains after calcination to remove the template (350°C) and subsequent carbonization (>600°C) to transform the resin into mesostructured carbons with high porosity (>800 m^2/g) (Fig. 65). Materials with varied pore size and packing are formed and controlled by the relative lengths of the PPO and PEO segments, as well as their concentration in the suspending solvent. Long-range order in the pores was observed via SAXS and TEM [172–174]. A similar strategy was used for the formation of carbon nanofibers from block copolymers based on polyacrylonitrile (PAN), a common precursor used in the formation of carbon nanofibers on both the laboratory and industrial scales. Block copolymers of PAN-b-PS were micellized in chloroform to prepare wormlike micellar aggregates (10–20 nm diameter) with PAN at the core (PAN DP = 20) [175]. Addition of free PAN homopolymer increased the micelle sizes 40–140 nm, resulting in much thicker carbon structures after carbonization.

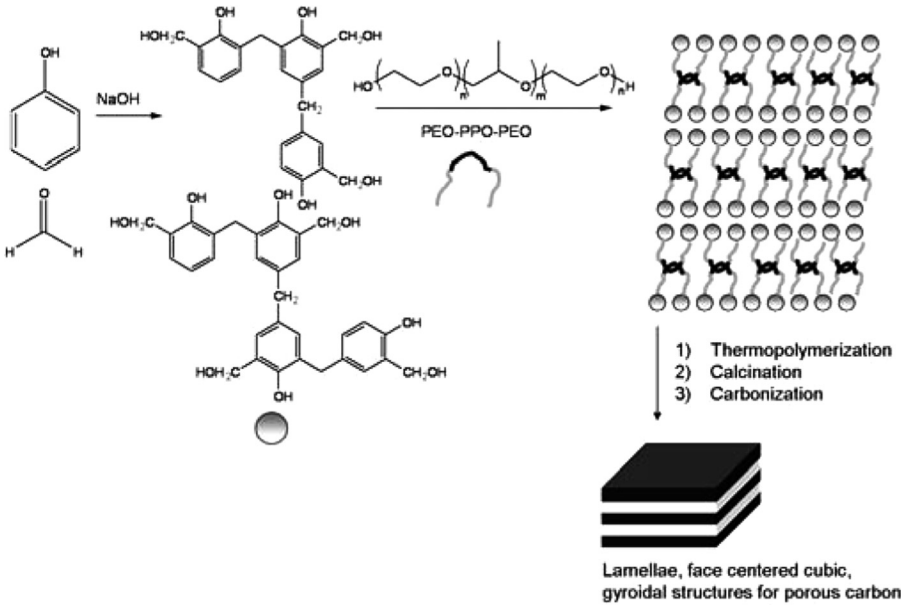

Figure 65. Micellar suspensions of PEO-b-PPO-b-PEO as templates for carbon structures derived from resorcinol precursors [172–174].

Block Copolymer Templates Containing Carbon Precursor Moieties

Our group has also utilized block copolymers containing PAN as a means of producing nanostructured carbon materials, with poly(*n*-butyl acrylate) (P*n*BA) serving as the primary sacrificial block due to its low glass transition temperature and significant immiscibility with PAN [176]. Both triblock PAN-b-P*n*BA-b-PAN [176] and diblock PAN-b-P*n*BA copolymers [177] were prepared by ATRP from P*n*BA macroinitaitors, [178,179] both difunctional and monofunctional and cast onto silica substrates from solution in DMF. The polymers self-segregated to form spheres (triblock copolymers), cylinders, and lamella (diblock copolymers with >15 wt% PAN), which could then be crosslinked through oxidative stabilization of the PAN domains at 250°C followed by pyrolysis and carbonization at 800°C. Significant orientation in the PAN domains (and subsequent carbon) was induced by using the zone-casting method of film preparation, with spacings of $\sim$37 nm before and after carbonization for both cylindrical and lamellar structures (Fig. 66). These carbons were electrically conductive, with conductivities ranging from $10 - 10^3$ S/cm when the pyrolysis temperatures were between 500 and 900°C [177]. PAN homopolymer grafted from silica nanoparticles and subsequently pyrolyzed prior to removal of the silica nanoparticles via etching was another method of producing porous/mesoporous carbon structures ($\sim$450 m^2/g), though without the significant orientation offered by the use of block copolymers and zone-casting [180].

More complex polymer topologies were also investigated. Polymer brushes were prepared from a poly(2-(2-bromopropionyloxy)ethyl methacrylate) (PBPEM) backbone by block extending first with *n*BA using CuBr/CuBr2 and 4,4′-di(5-nonyl)-2,2′-bipyridine (dNbpy) in anisole, then with AN using $CuCl/CuCl_2$ and bpy in DMF (Fig. 67) [181]. Attempts at thermal stabilization and carbonization of these brushes resulted not in the formation of the anticipated carbon nanotube-like structures, but rather in the formation of individual carbon particles, a result of cleavage in the backbone and the disruption of the phase separated morphology upon brush collapse. However, chain extension of the brush copolymer side chains for a third time with *t*-butyl acrylate using $CuCl/CuCl_2$ and PMDETA with a subsequent hydrolysis of the *t*BA groups to give polyacrylic acid outer blocks provided a brush copolymer that is susceptible to crosslinking in the outer shell. This crosslinking was accomplished

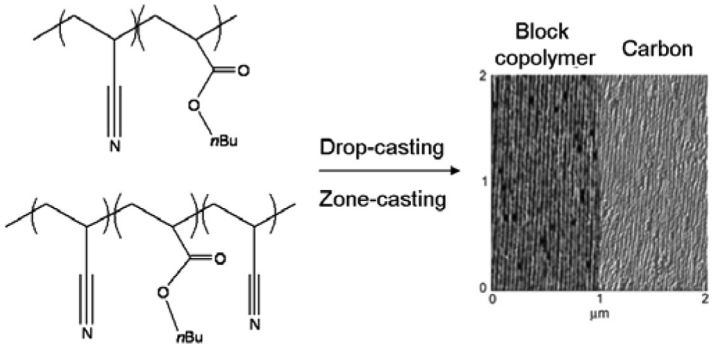

Figure 66. PAN-*b*-PBA and PAN-*b*-PBA-*b*-PAN block copolymers as precursors for nanostructured carbon films [176,177].

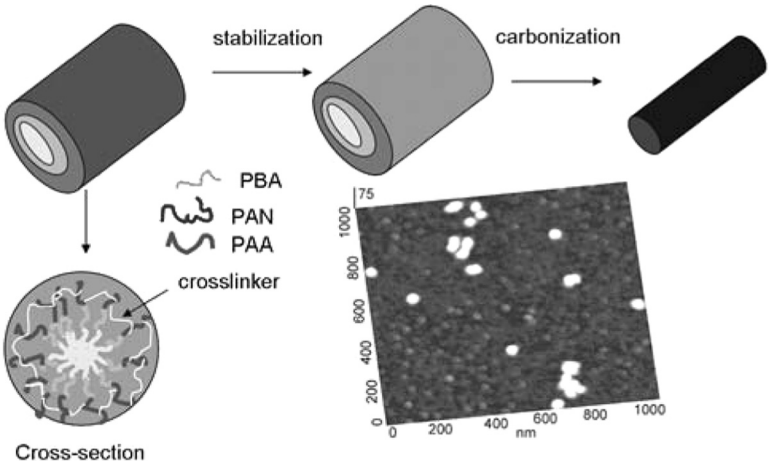

Figure 67. Brush block copolymers containing P*n*BA-b-PAN-b-PAA arms on a HEMA-derived backbone are crosslinked prior to stabilization and carbonization in order to prevent cleavage of the brush backbone during processing [181].

through the acidic PAA shell by using a diamine, 2,2′-(ethylenedioxy)-bis(ethylamine) as the crosslinking moiety with the aid of a water-soluble carbodiimide, (1-[3′-(dimethylamino)propyl]-3-ethylcarbodiimide methiodide). Subsequent stabilization and carbonization of the crosslinked brushes gave carbon structures containing a similar shape as the initial block brush copolymers, though the height was significantly decreased due to the low carbon yield from PAN (~7 nm vs 19 nm).

A similar crosslinking method was used by our group for the preparation of discrete carbon nanoparticles. A block copolymer consisting of P*t*BA and PAN was prepared by ATRP using CuCl/bpy as the catalyst (from a P*t*BA macroinitiator), hydrolyzed to PAA-b-PAN using anhydrous trifluoroacetic acid (TFA), and micellized by dissolution in DMF and dialysis against water [182]. These micelles, containing a PAN core and a PAA shell, were then crosslinked using the diamine/carbodiimide pair described above, and deposited on silica prior to stabilization and carbonization (Fig. 68). The resulting carbon nanostructures were of fairly uniform size and height as determined by tapping mode AFM, particularly at higher carbonization temperatures (900°C). All of the PAN-based carbon materials exhibit some amount of graphitic carbon, from analysis by Raman spectroscopy, though there is always a significant D-band component for disordered amorphous carbon, as well, a common factor in organically-derived carbon materials. Our group has also prepared spherical nanoparticles from PEO-b-PS block copolymer micelles and brush copolymers, where crosslinking through the PS domain with UV irradiation (253 nm) prior to pyrolysis resulted in discrete carbon nano-objects rather than decomposition of the PS domains, as is the case for uncrosslinked PS [183] (Fig. 69). In the brush copolymers, which contained a PAA shell over the PS-based core, the decomposition of the PAA during heat treatment resulted in the loss of the extended brush shape through longitudinal contraction, though the backbone itself was not cleaved during pyrolysis. The carbon derived from crosslinked PS also exhibited a mix of graphitic and amorphous carbon as exhibited by the presence of both D and G bands observed by Raman spectroscopy.

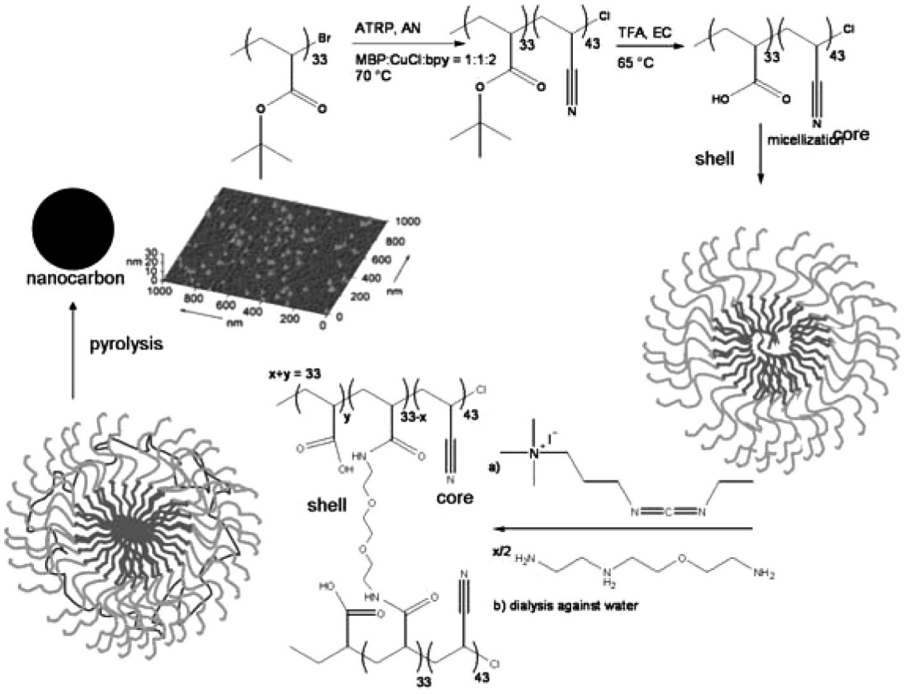

Figure 68. Shell-crosslinked micelles of PAN-b-PAA provide carbon nanospheres after stabilization and carbonization at temperatures >600°C [182].

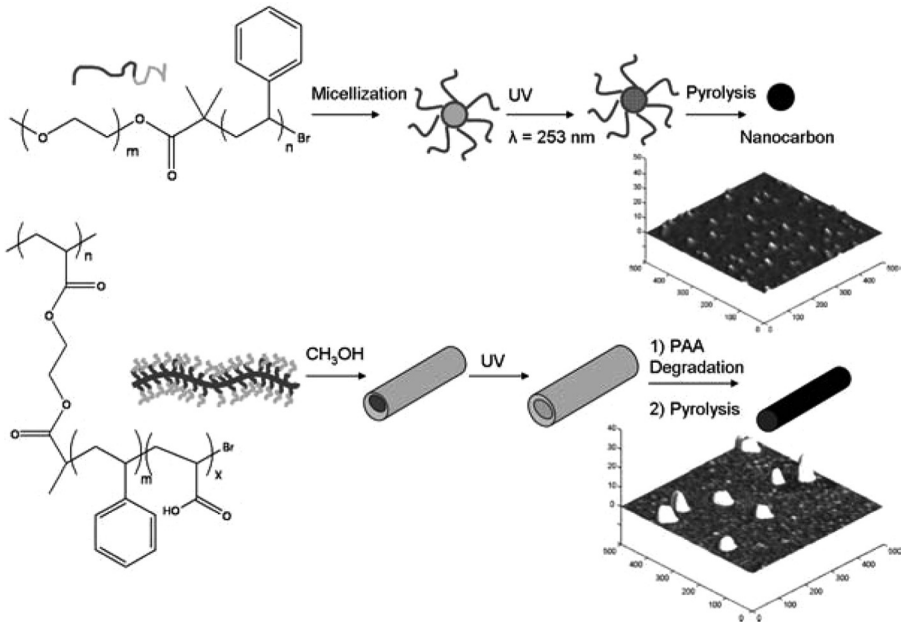

Figure 69. PS-b-PEO block copolymers and brush copolymers as precursors for carbon nanospheres and nanorods after UV-crosslinking of the PS domain prior to pyrolysis and carbonization [183].

Summary and Conclusions

Segmented copolymers can be used in multiple ways to modify the properties of conducting materials, from the incorporation of conducting and amorphous polymer segments into a linear polymer backbone, to grafting conjugated polymers from an amorphous backbone, to synthesizing conducting materials onto a self-assembled block copolymer template. Several methods of preparation are available, including controlled radical polymerization, cross-coupling reactions, and non-covalent interactions. These modifications improve solubility and ease the processing of conjugated materials, though maintaining the high conductivities of the pure polymers has proven to be challenging. ATRP and NMP are the two most prevalent methods for preparing block copolymers containing a conducting polymer segment and an amorphous polymer segment, because of the wide monomer selection and the ease of functionalizing conducting polymer end groups, especially with ATRP initiating moieties. Functionalization with NMP initiators is slightly more difficult, requiring the use of a butyllithium reagent to prepare the nitroxide end group, but has the added benefit not requiring a metal catalyst, resulting in no residual metal in the block copolymer, a significant advantage for certain applications, particularly photovoltaics. Conductivities in these types of block copolymers, particularly with regioregular polythiophenes, is high (1–10 S/cm), unlike the conductivities for discrete conducting nano-objects, which tend to fall in the range of 10^{-3} – 10^{-1} S/cm, depending on the conducting polymer used and the type of dopant (small molecule or polymeric) used. Graft copolymers are also easily prepared, either by end-capping a macroinitiator with a polymerizable conducting functionality like pyrrole or thiophene, or conversely by substituting an ATRP or other polymerization initiating functionality onto the conjugated polymer backbone. This method, in particular, provides materials with improved fluorescence properties because it prevents π-stacking and thus red-shifting in the solid state. Pure electrical conductivities, however, remain low due to high insulating polymer contents and lack of planarity in the conducting polymer grafts. The potential for self-assembled and stimuli-responsive materials in this field remains quite high and relatively unexplored, particularly with applications-directed research that incorporates stimuli-responsive block copolymers. The potential for using nanostructured carbon materials derived from block copolymers as components in energy storage devices like supercapacitors and lithium ion batteries is also quite high, though it is receiving increasing attention in the literature.

Acknowledgments

Grateful thanks are given to Dr. Bruno Dufour and Professor Tomasz Kowalewski for helpful discussions, as well as to NSF for funding (DMR 09-69301).

References

[1] Chiang, C. K., Fincher, C. R. Jr., Park, Y. W., Heeger, A. J., Shirakawa, H., Louis, E. J., Gau, S. C., & MacDiarmid, A. G. (1977). *Phys. Rev. Lett.*, *39*, 1098.
[2] Tourillon, G. & Garnier, F. (1982). *J. Electroanal. Chem. Interfacial Electrochem.*, *135*, 173.
[3] Wnek, G. E., Chien, J. C. W., Karasz, F. E., & Lillya, C. P. (1979). *Polymer*, *20*, 1441.

[4] Chien, J. C. W., Gooding, R. D., Karasz, F. E., Lillya, C. P., Wnek, G. E., & Yao, K. D. (1980). *Org. Coat. Plast. Chem.*, *43*, 886.
[5] Huang, W. S., Humphrey, B. D., & MacDiarmid, A. G. (1986). *J. Chem. Soc., Faraday Trans. 1*, *82*, 2385.
[6] MacDiarmid, A. G., Chiang, J. C., Richter, A. F., & Epstein, A. J. (1987). *Synth. Met.*, *18*, 285.
[7] Bolto, B. A., McNeill, R., & Weiss, D. E. (1963). *Aust. J. Chem.*, *16*, 1090.
[8] Diaz, A. F., Kanazawa, K. K., & Gardini, G. P. (1979). *J. Chem. Soc., Chem. Commun.*, *635*.
[9] MacDiarmid, A. G., Chiang, J. C., Huang, W., Humphrey, B. D., & Somasiri, N. L. D. (1985). *Mol. Cryst. Liq. Cryst.*, *125*, 309.
[10] Heeger, A. J., Kivelson, S., Schrieffer, J. R., & Su, W. P. (1988). *Rev. Mod. Phys.*, *60*, 781.
[11] Pron, A. & Rannou, P. (2001). *Prog. Polym. Sci.*, *27*, 135.
[12] Roux, C., Faid, K., & Leclerc, M. (1994). *Polym. News*, *19*, 6.
[13] Dao, L. H., Leclerc, M., Guay, J., & Chevalier, J. W. (1989). *Synth. Met.*, *29*, E377.
[14] Yang, S. M. & Chiang, J. H. (1991). *Synth. Met.*, *41*, 761.
[15] Francois, B. & Olinga, T. (1993). *Synth. Met.*, *57*, 3489.
[16] Cesar, B., Rawiso, M., Mathis, A., & Francois, B. (1997). *Synth. Met.*, *84*, 241.
[17] Francois, B., Widawski, G., Rawiso, M., & Cesar, B. (1995). *Synth. Met.*, *69*, 463.
[18] Grana, E., Katsigiannopoulos, D., Avgeropoulos, A., & Goulas, V. (2008). *Int. J. Polym. Anal. Charact.*, *13*, 108.
[19] Li, W., Maddux, T., & Yu, L. (1996). *Macromolecules*, *29*, 7329.
[20] Hempenius, M. A., Langeveld-Voss, B. M. W., van Haare, J. A. E. H., Janssen, R. A. J., Sheiko, S. S., Spatz, J. P., Moeller, M., & Meijer, E. W. (1998). *J. Am. Chem. Soc.*, *120*, 2798.
[21] Loewe, R. S., Khersonsky, S. M., & McCullough, R. D. (1999). *Adv. Mater.*, *11*, 250.
[22] Loewe, R. S., Ewbank, P. C., Liu, J., Zhai, L., & McCullough, R. D. (2001). *Macromolecules*, *34*, 4324.
[23] Stefan, M. C., Javier, A. E., Osaka, I., & McCullough, R. D. (2009). *Macromolecules*, *42*, 30.
[24] Iovu, M. C., Sheina, E. E., Gil, R. R., & McCullough, R. D. (2005). *Macromolecules*, *38*, 8649.
[25] Iovu, M. C., Jeffries-El, M., Zhang, R., Kowalewski, T., & McCullough, R. D. (2006). *J. Macromol. Sci., Part A: Pure Appl. Chem.*, *43*, 1991.
[26] Dai, C.-A., Yen, W.-C., Lee, Y.-H., Ho, C.-C., & Su, W.-F. (2007). *J. Am. Chem. Soc.*, *129*, 11036.
[27] Matyjaszewski, K. (1995). *J. Phys. Org. Chemi.*, *8*, 197.
[28] Matyjaszewski, K. (1997). *J. Macromol. Sci.-Pure & Applied Chem.*, *A34*, 1785.
[29] Jakubowski, W., Min, K., & Matyjaszewski, K. (2006). *Macromolecules*, *39*, 39.
[30] Jakubowski, W. & Matyjaszewski, K. (2006). *Ang. Chem.-Int. Ed.*, *45*, 4482.
[31] Matyjaszewski, K., Jakubowski, W., Min, K., Tang, W., Huang, J. Y., Braunecker, W. A., & Tsarevsky, N. V. (2006). *Proc. Nation. Acad. Sci. USA*, *103*, 15309.
[32] Pintauer, T. & Matyjaszewski, K. (2005). *Coord. Chem. Rev.*, *249*, 1155.
[33] Braunecker, W. A. & Matyjaszewski, K. (2007). *Prog. Polym. Sci.*, *32*, 93.
[34] Jakubowski, W. & Matyjaszewski, K. (2005). *Macromolecules*, *38*, 4139.
[35] Matyjaszewski, K. & Xia, J. (2001). *Chem. Rev.*, *101*, 2921.
[36] McCullough, L. A., Dufour, B., Tang, C., Zhang, R., Kowalewski, T. & Matyjaszewski, K. (2007). *Macromolecules*, *40*, 7745.
[37] Tsarevsky, N. V. & Matyjaszewski, K. (2007). *Chem. Rev.*, *107*, 2270.
[38] Wang, J.-S. & Matyjaszewski, K. (1995). *Macromolecules*, *28*, 7901.
[39] Matyjaszewski, K. & Tsarevsky, N. V. (2009). *Nat. Chem.*, *1*, 276.
[40] Hawker, C. J., Bosman, A. W., & Harth, E. (2001). *Chem. Rev.*, *101*, 3661.

[41] Moad, G., Rizzardo, E., & Solomon, D. H. (1982). *Macromolecules*, *15*, 909.
[42] Rizzardo, E. & Solomon, D. H. (1979). *Polym. Bull.*, *1*, 529.
[43] Debuigne, A., Poli, R., Jerome, C., Jerome, R., & Detrembleur, C. (2009). *Prog. Polym. Sci.*, *34*, 211.
[44] Mayadunne, R. T. A., Rizzardo, E., Chiefari, J., Chong, Y. K., Moad, G., & Thang, S. H. (1999). *Macromolecules*, *32*, 6977.
[45] Lowe, A. B. & McCormick, C. L. (2007). *Prog. Polym. Sci.*, *32*, 283.
[46] Chiefari, J., Chong, Y. K., Ercole, F., Krstina, J., Jeffery, J., Le, T. P. T., Mayadunne, R. T. A., Meijs, G. F., Moad, C. L., Moad, G., Rizzardo, E., & Thang, S. H. (1998). *Macromolecules*, *31*, 5559.
[47] Pavlidou, S. & Papaspyrides, C. D. (2008). *Prog. Polym. Sci.*, *33*, 1119.
[48] Bhadra, S., Khastgir, D., Singha, N. K., & Lee, J. H. (2009). *Prog. Polym. Sci.*, *34*, 783.
[49] Egbe, D. A. M., Carbonnier, B., Birckner, E., & Grummt, U.-W. (2009). *Prog. Polym. Sci.*, *34*, 1023.
[50] Deng, J., Wang, L., Liu, L., & Yang, W. (2009). *Prog. Polym. Sci.*, *34*, 156.
[51] Hamley, I. W. (2009). *Prog. Polym. Sci.*, *34*, 1161.
[52] He, D., Susanto, H., & Ulbricht, M. (2009). *Prog. Polym. Sci.*, *34*, 62.
[53] Lu, J., Yan, F., & Texter, J. (2009). *Prog. Polym. Sci.*, *34*, 431.
[54] Tomczak, N., Janczewski, D., Han, M., & Vancso, G. J. (2009). *Prog. Polym. Sci.*, *34*, 393.
[55] Sheiko, S. S., Sun, F. C., Randall, A., Shirvanyants, D., Rubinstein, M., Lee, H., & Matyjaszewski, K. (2006). *Nature*, *440*, 191.
[56] Tang, C. B., Kowalewski, T., & Matyjaszewski, K. (2003). *Macromolecules*, *36*, 1465.
[57] Kowalewski, T., Tsarevsky, N. V., & Matyjaszewski, K. (2002). *J. Am. Chem. Soc.*, *124*, 10632.
[58] Gao, H. & Matyjaszewski, K. (2009). *Prog. Polym. Sci.*, *34*, 317.
[59] Coca, S. & Matyjaszewski, K. (1997). *Macromolecules*, *30*, 2808.
[60] Ziegler, M. J. & Matyjaszewski, K. (2001). *Macromolecules*, *34*, 415.
[61] Oh, J. K., Drumright, R., Siegwart, D. J., & Matyjaszewski, K. (2008). *Prog. Polym. Sci.*, *33*, 448.
[62] Arehart, S. V. & Matyjaszewski, K. (1999). *Macromolecules*, *32*, 2221.
[63] Yagci, Y. & Tasdelen, M. A. (2006). *Prog. Polym. Sci.*, *31*, 1133.
[64] Coca, S., Paik, H. J., & Matyjaszewski, K. (1997). *Macromolecules*, *30*, 6513.
[65] Davis, K. A., Charleux, B. & Matyjaszewski, K. (2000). *J. Polym. Sci., Part A: Polym. Chem.*, *38*, 2274.
[66] Gaynor, S. G. & Matyjaszewski, K. (1997). *Macromolecules*, *30*, 4241.
[67] Matyjaszewski, K., Beers, K. L., Kern, A., & Gaynor, S. G. (1998). *J. Polym. Sci., Polym. Chem.*, *36*, 823.
[68] Matyjaszewski, K., Jo, S. M., Paik, H.-J. & Shipp, D. A. (1999). *Macromolecules*, *32*, 6431–6438.
[69] Shinoda, H. & Matyjaszewski, K. (2001). *Macromolecules*, *34*, 6243.
[70] Pyun, J. & Matyjaszewski, K. (2000). *Macromolecules*, *33*, 217.
[71] Min, K. & Matyjaszewski, K. (2009). *Cent. Eur. J. Chem.*, *7*, 657.
[72] Liu, J., Sheina, E., Kowalewski, T., & McCullough, R. D. (2002). *Angew. Chem., Int. Ed.*, *41*, 329.
[73] Iovu, M. C., Jeffries-El, M., Sheina, E. E., Cooper, J. R., & McCullough, R. D. (2005). *Polymer*, *46*, 8582.
[74] Sauve, G. & McCullough, R. D. (2007). *Adv. Mater.*, *19*, 1822.
[75] Li, B., Sauve, G., Iovu, M. C., Jeffries-El, M., Zhang, R., Cooper, J., Santhanam, S., Schultz, L., Revelli, J. C., Kusne, A. G., Kowalewski, T., Snyder, J. L., Weiss, L. E., Fedder, G. K., McCullough, R. D., & Lambeth, D. N. (2006). *Nano Lett.*, *6*, 1598.
[76] Shipp, D. A., Wang, J.-L., & Matyjaszewski, K. (1998). *Macromolecules*, *31*, 8005.
[77] Iovu, M. C., Zhang, R., Cooper, J. R., Smilgies, D. M., Javier, A. E., Sheina, E. E., Kowalewski, T., & McCullough, R. D. (2007). *Macromol. Rapid Commun.*, *28*, 1816.

[78] Craley, C. R., Zhang, R., Kowalewski, T., McCullough, R. D., & Stefan, M. C. (2009). *Macromol. Rapid Commun.*, *30*, 11.
[79] De Cuendias, A., Le Hellaye, M., Lecommandoux, S., Cloutet, E., & Cramail, H. (2005). *J. Mater. Chem.*, *15*, 3264.
[80] Urien, M., Erothu, H., Cloutet, E., Hiorns, R. C., Vignau, L., & Cramail, H. (2008). *Macromolecules*, *41*, 7033.
[81] Alkan, S., Toppare, L., Hepuzer, Y., & Yagci, Y. (2001). *Synth. Met.*, *119*, 133.
[82] Mecerreyes, D., Pomposo, J. A., Bengoetxea, M., & Grande, H. (2000). *Macromolecules*, *33*, 5846.
[83] Tsolakis, P. K. & Kallitsis, J. K. (2003). *Chem.–Eur. J.*, *9*, 936.
[84] Chochos, C. L., Tsolakis, P. K., Gregoriou, V. G., & Kallitsis, J. K. (2004). *Macromolecules*, *37*, 2502.
[85] Yu, X.-F., Lu, S., Ye, C., Li, T., Liu, T., Liu, S., Fan, Q., Chen, E.-Q., & Huang, W. (2006). *Macromolecules*, *39*, 1364.
[86] Iovu, M. C., Craley, C. R., Jeffries-El, M., Krankowski, A. B., Zhang, R., Kowalewski, T., & McCullough, R. D. (2007). *Macromolecules*, *40*, 4733.
[87] Stalmach, U., De Boer, B., Post, A. D., Van Hutten, P. F., & Hadziioannou, G. (2001). *Angew. Chem., Int. Ed.*, *40*, 428.
[88] Van De Wetering, K., Brochon, C., Ngov, C., & Hadziioannou, G. (2006). *Macromolecules*, *39*, 4289.
[89] de Boer, B., Stalmach, U., van Hutten, P. F., Melzer, C., Krasnikov, V. V., & Hadziioannou, G. (2001). *Polymer*, *42*, 9097.
[90] Stalmach, U., de Boer, B., Videlot, C., van Hutten, P. F., & Hadziioannou, G. (2000). *J. Am. Chem. Soc.*, *122*, 5464.
[91] Van der Veen, M. H., De Boer, B., Stalmach, U., Van de Wetering, K. I., & Hadziioannou, G. (2004). *Macromolecules*, *37*, 3673.
[92] Heiser, T., Adamopoulos, G., Brinkmann, M., Giovanella, U., Ould-Saad, S., Brochon, C., van de Wetering, K., & Hadziioannou, G. (2006). *Thin Solid Films*, *511–512*, 219.
[93] Richard, F., Brochon, C., Leclerc, N., Eckhardt, D., Heiser, T., & Hadziioannou, G. (2008). *Macromol. Rapid Commun.*, *29*, 885.
[94] Barrau, S., Heiser, T., Richard, F., Brochon, C., Ngov, C., van de Wetering, K., Hadziioannou, G., Anokhin, D. V., & Ivanov, D. A. (2008). *Macromolecules*, *41*, 2701.
[95] Zhang, Q., Cirpan, A., Russell, T. P., & Emrick, T. (2009). *Macromolecules*, *42*, 1079.
[96] Ball, Z. T., Sivula, K., & Frechet, J. M. J. (2006). *Macromolecules*, *39*, 70.
[97] Sivula, K., Ball, Z. T., Watanabe, N., & Frechet, J. M. J. (2006). *Adv. Mater.*, *18*, 206.
[98] Radano, C. P., Scherman, O. A., Stingelin-Stutzmann, N., Mueller, C., Breiby, D. W., Smith, P., Janssen, R. A. J., & Meijer, E. W. (2005). *J. Am. Chem. Soc.*, *127*, 12502.
[99] Boudouris, B. W., Frisbie, C. D., & Hillmyer, M. A. (2008). *Macromolecules*, *41*, 67.
[100] Kilbinger, A. F. M., & Feast, W. J. (2000). *J. Mater. Chem.*, *10*, 1777.
[101] Cik, G., Krajcovic, J., Hubinova, M., Kristin, J., Cerven, I., & Sersen, F. (2004). *Synth. Met.*, *140*, 301.
[102] Henze, O. & Feast, W. J. (2003). *J. Mater. Chem.*, *13*, 1274.
[103] Kinlen, P. J., Frushour, B. G., Ding, Y., & Menon, V. (1999). *Synth. Met.*, *101*, 758.
[104] Yan, L. & Tao, W. (2007). *J. Polym. Sci., Part A: Polym. Chem.*, *46*, 12.
[105] Hua, F. & Ruckenstein, E. (2004). *J. Polym. Sci., Part A: Polym. Chem.*, *42*, 2179.
[106] Huang, L., Hu, J., Lang, L., Wang, X., Zhang, P., Jing, X., Wang, X., Chen, X., Lelkes, P. I., MacDiarmid, A. G., & Wei, Y. (2007). *Biomaterials*, *28*, 1741.
[107] Ding, C., Wang, Y., & Zhang, S. (2007). *Eur. Polym. J.*, *43*, 4244.
[108] Carone, E., D'Ilario, L., & Martinelli, A. (2002). *J. Appl. Polym. Sci.*, *83*, 857.
[109] Liu, J.-Y., Yang, C.-C., & Wang, Y.-Z. (2007). *J. Appl. Polym. Sci.*, *103*, 3803.
[110] Yagci, Y. & Toppare, L. (2003). *Polym. Int.*, *52*, 1573.
[111] Kizilyar, N., Toppare, L., Onen, A., & Yagci, Y. (1998). *Polym. Bull.*, *40*, 639.
[112] Yagci, Y. & Toppare, L. (2000). *Macromol. Symp.*, *157*, 29.

[113] Gursel, A., Alkan, S., Toppare, L., & Yagci, Y. (2003). *React. Funct. Polym.*, *57*, 57.
[114] Kalaycioglu, E., Toppare, L., Yagci, Y., Harabagiu, V., Pintela, M., Ardelean, R., & Simionescu, B. C. (1998). *Synth. Met.*, *97*, 7.
[115] Bozkurt, A., Parlak, M., Ercelebi, C., & Toppare, L. (2002). *J. Appl. Polym. Sci.*, *85*, 52.
[116] Biran, C., Toppare, L., Tincer, T., Yagci, Y., & Harabagiu, V. (2002). *J. Appl. Polym. Sci.*, *86*, 1663.
[117] Sun, X.-L., He, W.-D., Li, J., He, N., Han, S.-C., & Li, L.-Y. (2008). *J. Polym. Sci., Part A: Polym. Chem.*, *46*, 6950.
[118] Mecerreyes, D., Stevens, R., Nguyen, C., Pomposo, J. A., Bengoetxea, M., & Grande, H. (2002). *Synth. Met.*, *126*, 173.
[119] Jerome, C., Martinot, L., Louette, P., & Jerome, R. (2000). *Macromol. Symp.*, *153*, 305.
[120] Oztemiz, S., Toppare, L., Onen, A., & Yagci, Y. (2000). *J. Macromol. Sci., Pure Appl. Chem., A37*, *277*.
[121] Shustak, G., Gadzinowski, M., Slomkowski, S., Domb, A. J., & Mandler, D. (2007). *New J. Chem.*, *31*, 163.
[122] Kalaycioglu, E., Toppare, L., & Yagci, Y. (2000). *Synth. Met.*, *108*, 1.
[123] Cirpan, A., Alkan, S., Toppare, L., Hepuzer, Y., & Yagci, Y. (2002). *J. Polym. Sci., Part A: Polym. Chem.*, *40*, 4131.
[124] Yilmaz, F., Sel, O., Guner, Y., Toppare, L., Hepuzer, Y., &Yagci, Y. (2004). *J. Macromol. Sci., Pure Appl. Chem.*, *A41*, 401.
[125] Park, Y. H. & Park, S. B. (2002). *Synth. Met.*, *128*, 229.
[126] Bae, W. J., Kim, K. H., Jo, W. H., & Park, Y. H. (2005). *Macromolecules*, *38*, 1044.
[127] Costanzo, P. J. & Stokes, K. K. (2002). *Macromolecules*, *35*, 6804.
[128] Shen, J. & Ogino, K. (2005). *Chem. Lett.*, *34*, 1616.
[129] Economopoulos, S. P., Chochos, C. L., Gregoriou, V. G., Kallitsis, J. K., Barrau, S., & Hadziioannou, G. (2007). *Macromolecules*, *40*, 921.
[130] Chen, X., Gholamkhass, B., Han, X., Vamvounis, G., & Holdcroft, S. (2007). *Macromol. Rapid Commun.*, *28*, 1792.
[131] Li, Z. F. & Ruckenstein, E. (2003). *J. Colloid Interface Sci.*, *264*, 370.
[132] Petrov, P., Mokreva, P., Tsvetanov, C. B., & Terlemezyan, L. (2008). *Colloid Polym. Sci.*, *286*, 691.
[133] Xu, F. J., Xu, D., Kang, E. T., & Neoh, K. G. (2004). *J. Mater. Chem.*, *14*, 2674.
[134] Soares, B. G. & Leyva, M. E. (2007). *Macromol. Mater. Eng.*, *292*, 354.
[135] Ruckenstein, E. & Sun, Y. (1995). *Synth. Met.*, *74*, 107.
[136] Souza, F. G., Soares, B. G., Mantovani, G. L., Manjunath, A., Somashekarappa, H., Somashekar, R., & Siddaramaiah. (2006). *Polymer*, *47*, 2163.
[137] Xie, H.-Q., Ma, Y.-M., & Guo, J.-S. (1998). *Polymer*, *40*, 261.
[138] Xie, H.-Q. & Ma, Y.-M. (2000). *J. Appl. Polym. Sci.*, *77*, 2156.
[139] Sheiko, S. S., Prokhorora, S. A., Beers, K. L., Matyjaszewski, K., Potemkin, I. I., Khokhlor, A. R., & Moeller, M. (2001). *Macromolecules*, *34*, 8354–8360.
[140] de Jesus, M. C., Weiss, R. A., & Hahn, S. F. (1998). *Macromolecules*, *31*, 2230.
[141] Yoo, S. I., Sohn, B.-H., Zin, W.-C., & Jung, J. C. (2004). *Langmuir*, *20*, 10734.
[142] Goren, M. & Lennox, R. B. (2001). *Nano Lett.*, *1*, 735.
[143] Selvan, S. T., Spatz, J. P., Klok, H. A., & Moeller, M. (1998). *Adv. Mater.*, *10*, 132.
[144] Selvan, S. T. (1998). *Chem. Commun.*, *351*.
[145] Ishizu, K., Honda, K., Kanbara, T., & Yamamoto, T. (1994). *Polymer*, *35*, 4901.
[146] Lee, D. H., Chang, J. A., & Kim, J. K. (2006). *J. Mater. Chem.*, *16*, 4575.
[147] Ishizu, K., Honda, K., & Saito, R. (1996). *Polymer*, *37*, 3965.
[148] Ishizu, K., Tsubaki, K., & Uchida, S. (2002). *Macromolecules*, *35*, 10193.
[149] Mezzenga, R., Ruokolainen, J., Fredrickson, G. H., Kramer, E. J., Moses, D., Heeger, A. J., & Ikkala, O. (2003). *Science*, *299*, 1872.
[150] McCullough, L. A., Dufour, B., & Matyjaszewski, K. (2009). *J. Polym. Sci., Part A: Polym. Chem.*, *47*, 5386.

[151] McCullough, L. A., Dufour, B., & Matyjaszewski, K. *Macromolecules*, ACS ASAP.
[152] McCullough, L. A., Dufour, B., & Matyjaszewski, K. (2009). *Macromolecules*, *42*, 8129.
[153] Li, X., Tian, S., Ping, Y., Kim, D. H., & Knoll, W. (2005). *Langmuir*, *21*, 9393.
[154] Beattie, D., Wong, K. H., Williams, C., Poole-Warren, L. A., Davis, T. P., Barner-Kowollik, C., & Stenzel, M. H. (2006). *Biomacromolecules*, *7*, 1072.
[155] Maeda, Y., Shimoi, Y., & Ogino, K. (2005). *Polym. Bull.*, *53*, 315.
[156] Lee, J. I., Cho, S. H., Park, S.-M., Kim, J. K., Kim, J. K., Yu, J.-W., Kim, Y. C., & Russell, T. P. (2008). *Nano Lett.*, *8*, 2315.
[157] Yang, J., Xiao, Y., & Martin, D. C. (2002). *Mater. Res. Soc. Symp. Proc.*, *734*, 187.
[158] Wolf, J. H. & Hillmyer, M. A. (2003). *Langmuir*, *19*, 6553.
[159] Zalusky, A. S., Olayo-Valles, R., Wolf, J. H., & Hillmyer, M. A. (2002). *J. Am. Chem. Soc.*, *124*, 12761.
[160] Zalusky, A. S., Olayo-Valles, R., Taylor, C. J., & Hillmyer, M. A. (2001). *J. Am. Chem. Soc.*, *123*, 1519.
[161] Johnson, B. J. S., Wolf, J. H., Zalusky, A. S., & Hillmyer, M. A. (2004). *Chem. Mater.*, *16*, 2909.
[162] Zhou, F., Liu, W., Hao, J., Xu, T., Chen, M., & Xue, Q. (2003). *Adv. Funct. Mater.*, *13*, 938.
[163] Bucholz, T., Sun, Y., & Loo, Y.-L. (2008). *J. Mater. Chem.*, *18*, 5835.
[164] Sapurina, I., Stejskal, J., & Tuzar, Z. (2001). *Colloids Surf., A*, *180*, 193.
[165] Sonmez, H. B., Sonmez, G., Senkal, B. F., Sarac, A. S., & Bicak, N. (2003). *Synth. Met.*, *807*, 135–136.
[166] Wang, M., Kumar, S., Lee, A., Felorzabihi, N., Shen, L., Zhao, F., Froimowicz, P., Scholes, G. D., & Winnik, M. A. (2008). *J. Am. Chem. Soc.*, *130*, 9481.
[167] Lee, D. H., Shin, D. O., Lee, W. J., & Kim, S. O. (2008). *Adv. Mater.*, *20*, 2480.
[168] Lee, D.-H., Shin, D.-O., Lee, W.-J., & Kim, S. O. (2008). *J. Nanosci. Nanotechnol.*, *8*, 5571.
[169] Rodriguez, A. T., Chen, M., Chen, Z., Brinker, C. J., & Fan, H. (2006). *J. Am. Chem. Soc.*, *128*, 9276.
[170] Rodriguez, A. T., Li, X., Wang, J., Steen, W. A., & Fan, H. (2007). *Adv. Funct. Mater.*, *17*, 2710.
[171] Soininen, A., Valkama, S., Nykaenen, A., Laiho, A., Kosonen, H., Mezzenga, R., & Ruokolainen, J. (2007). *Chem. Mater.*, *19*, 3093.
[172] Huang, Y., Cai, H., Yu, T., Zhang, F., Zhang, F., Meng, Y., Dong, G., Wan, Y., Sun, X., Tu, B., & Zhao, D. (2007). *Angew. Chem., Int. Ed.*, *46*, 1089.
[173] Meng, Y., Gu, D., Zhang, F., Shi, Y., Cheng, L., Feng, D., Wu, Z., Chen, Z., Wan, Y., Stein, A., & Zhao, D. (2006). *Chem. Mater.*, *18*, 4447.
[174] Wang, X., Liang, C., & Dai, S. (2008). *Langmuir*, *24*, 7500.
[175] Lazzari, M., Scalarone, D., Hoppe, C. E., Vazquez-Vazquez, C., & Lopez-Quintela, M. A. (2007). *Chem. Mater.*, *19*, 5818.
[176] Kowalewski, T., Tsarevsky, N. V., & Matyjaszewski, K. (2002). *J. Am. Chem. Soc.*, *124*, 10632.
[177] Tang, C., Tracz, A., Kruk, M., Zhang, R., Smilgies, D.-M., Matyjaszewski, K., & Kowalewski, T. (2005). *J. Am. Chem. Soc.*, *127*, 6918.
[178] Tang, C., Kowalewski, T., & Matyjaszewski, K. (2003). *Macromolecules*, *36*, 1465.
[179] Tang, C., Kowalewski, T., & Matyjaszewski, K. (2003). *Macromolecules*, *36*, 8587.
[180] Tang, C., Bombalski, L., Kruk, M., Jaroniec, M., Matyjaszewski, K., & Kowalewski, T. (2008). *Adv. Mater.*, *20*, 1516.
[181] Tang, C., Dufour, B., Kowalewski, T., & Matyjaszewski, K. (2007). *Macromolecules*, *40*, 6199.
[182] Tang, C., Qi, K., Wooley, K. L., Matyjaszewski, K., & Kowalewski, T. (2004). *Angew. Chem., Int. Ed.*, *43*, 2783.
[183] Huang, J., Tang, C., Lee, H., Kowalewski, T., & Matyjaszewski, K. (2007). *Macromol. Chem. Phys.*, *208*, 2312.